NRIAG JOURNAL OF ASTRONOMY AND GEOPHYSICS
2022, VOL. 11, NO. 1, 81–112
https://doi.org/10.1080/20909977.2021.1953297

OPEN ACCESS Check for updates

Pre-foundation geophysical investigation of a site for structural development in Oka, Nigeria

Omowumi Ademila

Department of Earth Sciences, Adekunle Ajasin University, Akungba-Akoko, Nigeria

ABSTRACT

Frequency of structural failure globally has necessitated geophysical investigation of subsurface geology of a site for engineering construction works. Combined very low frequency electromagnetic (VLF-EM) and electrical resistivity methods were used to provide detailed information on subsoil profile for documentation and references for durable and sustainable construction works. Thirteen traverses were established from which geophysical data were acquired. Major conductive geological interfaces suspected to be faults/fractured zones were identified from the plots of VLF-EM data. These points serve as 50 sounding stations further investigated using Schlumberger electrode array with vertical electrical sounding technique and electrical resistivity imaging on selected four traverses of the site. The acquired data were processed, inverted and interpreted. VLF-EM 2-D inverted models revealed conductive zones at some locations suggesting incompetent zones, responsible for structural instability. Saturated clayey subsoil and uneven bedrock topography with depressions at some points could cause differential settling which has negative impact on engineering structures. Structural failure may arise from existence of concealed geological structures, deep weathering/fractured bedrock, heterogeneous and structurally deformed (F1–F16) subsurface geological setting. Thus, classified unstable sections are considered priority in structural design and construction to mitigate unforeseen challenges. Deep foundations in form of piers and piles are encouraged to avert structural failure.

ARTICLE HISTORY
Received 23 February 2021
Revised 18 May 2021
Accepted 5 July 2021

KEYWORDS
Electrical resistivity investigation; Pre-foundation studies; Site characterisation; Structural failure; Very low frequency electromagnetic method (VLF-EM)

1. Introduction

Geophysical methods are widely applied in engineering-geological survey to provide quality information on the nature of subsoil, geologic sequence and structures. These methods offer valuable information concerning the early discovery of possible risky subsurface settings. The threat to civil engineering works are basically from concealed near surface; fractures, cavities, buried stream channels, sheared zones, voids, sink holes and inhomogeneities in the subsurface materials. Also, information regarding the geologic condition of the area is very important for safety of building foundations. Geophysical methods have been effectively used in near-surface engineering and foundation assessment (Sharma 1997; Ademila 2015). Electromagnetic and electrical methods among others are valuable tools for geo-engineering investigations to confirm the competence of foundation subsurface structures. Subsurface exploration is a vital step from which foundation stability response is acquired for the design and construction of sustainable civil engineering works (Oluwafemi and Oladunjoye 2013; Ademila 2015). Failure of civil engineering works makes no news as this happens on a daily basis in different geologic settings throughout the nation. The understanding of the properties and parameters of subsurface materials (rocks or soils) from measurements made at the surface of the earth provide subsurface information in solving engineering infrastructure problems. Civil engineering structures in Nigeria are constructed with no detailed information of the subsoil which acts as basic geomaterial upon which the foundations of these structures would be placed for support and stability. Structural failure is usually linked to substandard structural materials and poor plan with no consideration of the subsoil (Ademila 2018). Combined geophysical investigations provide the basic information of the subsurface sequence and structural disposition necessary for foundation design. This is to offer the assurance of the suitability of the subsoil and the type of foundation for building construction. The intrinsic reason for structural failure lies on inadequate understanding of geophysical and hydrogeological information as regards the nature/type of soils, geologic sequence and structures, which are the water bearing units detrimental to stability of structures. These are paramount to effectively characterise the heterogeneous subsoil properties beneath the engineering site and to enhance successful structural development. Site response studies involving geophysical approach serve as an efficient step of characterising subsurface geology of site for the design of civil engineering works from

CONTACT Omowumi Ademila omowumi.ademila@aaua.edu.ng Department of Earth Sciences, Adekunle Ajasin University, Akungba-Akoko, Nigeria

© 2022 The Author(s). Published by Informa UK Limited, trading as Taylor & Francis Group.
This is an Open Access article distributed under the terms of the Creative Commons Attribution License (http://creativecommons.org/licenses/by/4.0/), which permits unrestricted use, distribution, and reproduction in any medium, provided the original work is properly cited.

which detailed structural nature of the subsurface are generated (Khalil et al. 2010). This also makes provision for early discovery of potentially unstable subsurface conditions and accounts for the effects of spatial variability of the subsurface which can hamper soil-structure interaction and cause structural failure (Capilleri et al. 2018; Chandran and Anbazhagan 2020). Electromagnetic (VLF-EM) and electrical resistivity methods being non-destructive from which measurements are made at the surface of the earth have been effectively used for groundwater exploration, mapping and detecting groundwater contamination, mineral exploration, engineering site investigations and related geological structures, landfill and contaminant characterisation, archaeological prospecting and foundation instability analysis (Bayrak 2002; Cardarelli et al. 2007; Oluwafemi 2012; Oluwafemi and Oladunjoye 2013; Ademila 2015, 2021; Pazzi et al. 2016; Ademila and Ololade 2018; Ademila et al. 2020). This has been supported with computing power and image processing algorithms for inversion of geophysical data sets for subsurface images and evaluation of geoelectric parameters (Loke 2000). The quest for stable and sustainable structural development prompted the need for subsurface characterisation of engineering site. Oka-Akoko, the study area being in Basement Complex geological setting requires a detailed knowledge of the geological and geo-engineering materials, nature of subsurface conditions of the construction site due to the heterogeneity and variations in the subsurface environments. This becomes imperative for development as the subsoil would interact with the structure on site. Hence, this research used combined very low frequency electromagnetic (VLF-EM) and electrical resistivity techniques to characterise subsurface geological disposition of the engineering site with the aim of identifying subsurface geological structures with possible engineering threat to proposed building projects. This will help in decision making on the suitability of the site for construction and to design effective structural foundations for sustainable building constructions. The sufficient subsurface data acquired would also give detailed information on the foundation type and dimensions of the proposed buildings. This serves as a preconstruction investigation of a site for structures in order to prevent tilting and sudden collapse of buildings with resultant needless loss of lives and valuables. These data would also guide the suitable location of borehole site in the area to support its potential groundwater development.

2. Area of study (location and geology)

The study area in Akoko Southwest of Ondo State, Nigeria, is between latitudes 7° 25′ N and 7° 30′ N and longitudes 5° 45′ E and 5° 50′ E (Figure 1) with approximately area of 42 square kilometres. It has boundary with Ugbe/Isua towards north, Ikun towards south west, Akungba towards southeast and Ayegunle/Oba-Akoko to the south. The topography of the area is distinguished by highlands in the form of hills and inselbergs and lowlands in the form of plains and valleys. It has highest elevation approximately 600 m (Figure 1). It is one of the most populous towns in Ondo Northern Senatorial district. The area is accessible through different footpaths and good road network particularly the Owo-Akungba-Iwaro and Isua-Ibillo-Okene roads. It is characterised by tropical rainforest belt of Nigeria having two distinct (rainy and dry) seasons. The mean annual rainfall is about 1650 mm with mean annual temperature, 27.5°C and relative humidity of over 70%. The vegetation is evergreen rainforest type characterised by some trees. The study area is drained mainly by Rivers Ogbehli, Agbagbara, Asawa and Ojomirin with a dendritic drainage network pattern. The survey site (National Open University of Nigeria) in Oka-Akoko is approximately 2.64 km^2. Lithologically, the area is characterised by migmatite-gneiss-quartzite complex of crystalline rocks of Nigeria (Rahaman 1989). Field mapping exercise showed granite gneiss, grey gneiss and older granite rocks (Figure 2) and minor occurrences of pegmatite, aplite and charnockitic rocks as the main lithologic units in the area. The grey and granite gneisses dominant the area (Figure 2). Rocks in the area are subjected to several phases of deformation with resultant hydrogeological structures, which aid groundwater accumulation and serve as groundwater prospective zones in the area. Aquiferous zones in basement complex constitute the weathered and fissured/fractured bedrock from which residents derived water for use through hand dug wells having depth in the range 2.87–12.43 m. This shallow depth of water in the area could contribute to structural failure as a result of interaction of foundation subsoils with water (Ademila, 2019).

3. Materials and methods

This study includes thorough geological mapping exercise to establish the lithologic rock units of the area. The coordinates and elevations of each location were measured with a global positioning system (GPS). This is done in an attempt to produce the geological map and geophysical field layout map of the survey area. A total of 13 traverses were established with seven traverses orienting approximately in NW–SE and six traverses in NE–SW directions along which VLF-EM and electrical resistivity data were acquired (Figure 3). The VLF-EM measurements were conducted on the 13 traverses with 10 m station interval with ABEM WADI VLF system and the length in the range 250 to 600 m (Figure 3). These traverses were set

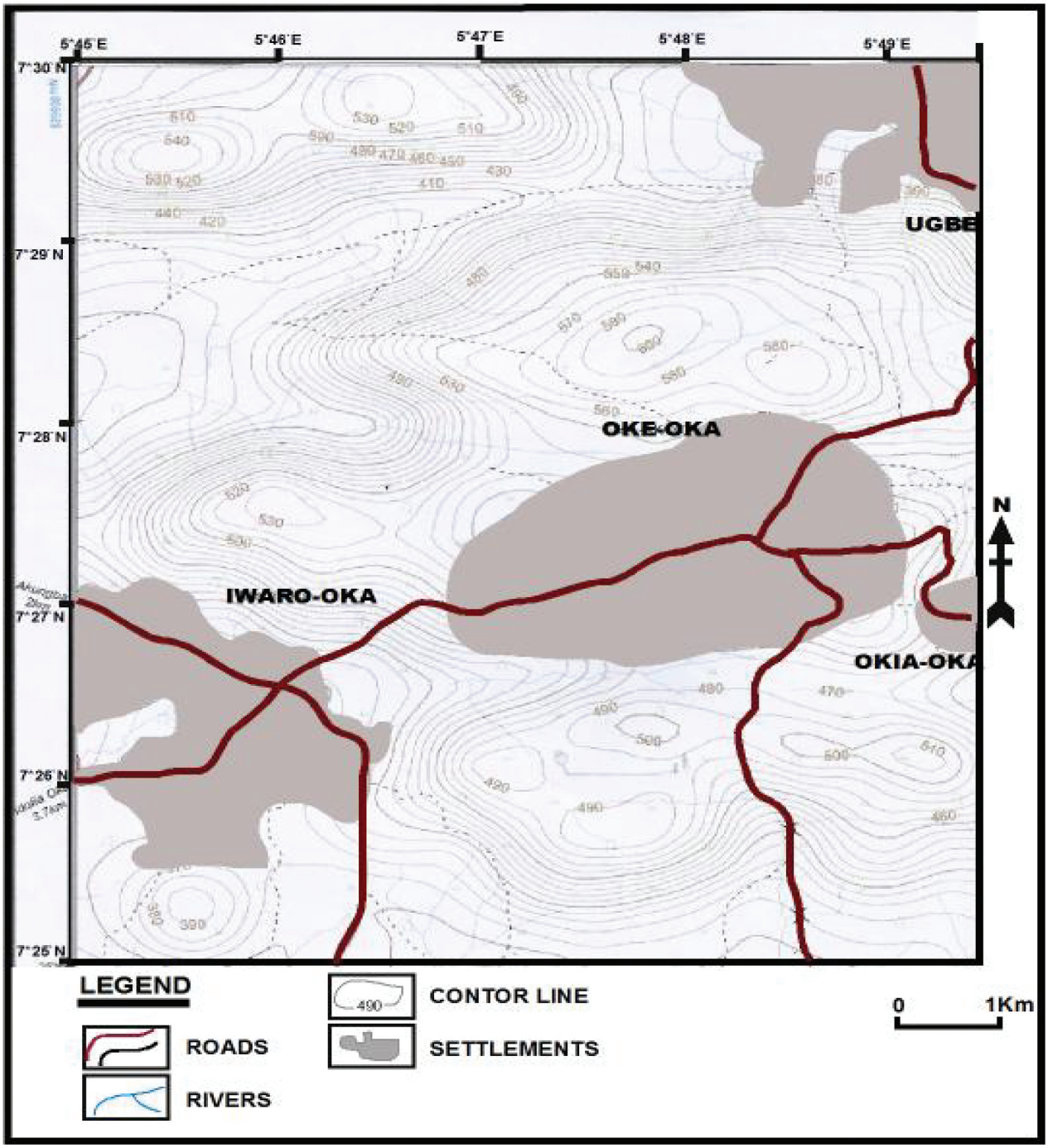

Figure 1. Topographical map of Oka-Akoko.

to guarantee adequate conductor coupling and the VLF instrument measures the horizontal (H_p) and vertical (H_s) components of magnetic field in the form of real and imaginary parts of vertical magnetic field component. These data are displayed as profiles by plotting raw real and filtered real components against distance (Figures 4a–16a). The qualitative interpretation of the profile presents the conductive zones in the subsurface at intersection of the raw real and positive peaks of the filtered real (Nabighian 1988). These data which are indicative of near surface geologic structures were thereafter processed also for qualitative interpretation. They were presented as inverted pseudosections with the aid of KH Filt software (Pirttijarvi 2004). The electrical resistivity method employed Schlumberger vertical electrical sounding (VES) technique and ABEM 1000 terrameter system was engaged to acquire VES data with electrode spread (AB/2) in the range 1–150 m. Fifty (50) VES acquired across the site were the major conductive points delineated from VLF survey along the traverses (Figure 3), to investigate the vertical changes in the resistivity distribution. The acquired data were processed manually (plot of apparent resistivity versus AB/2 on bi-log graph).

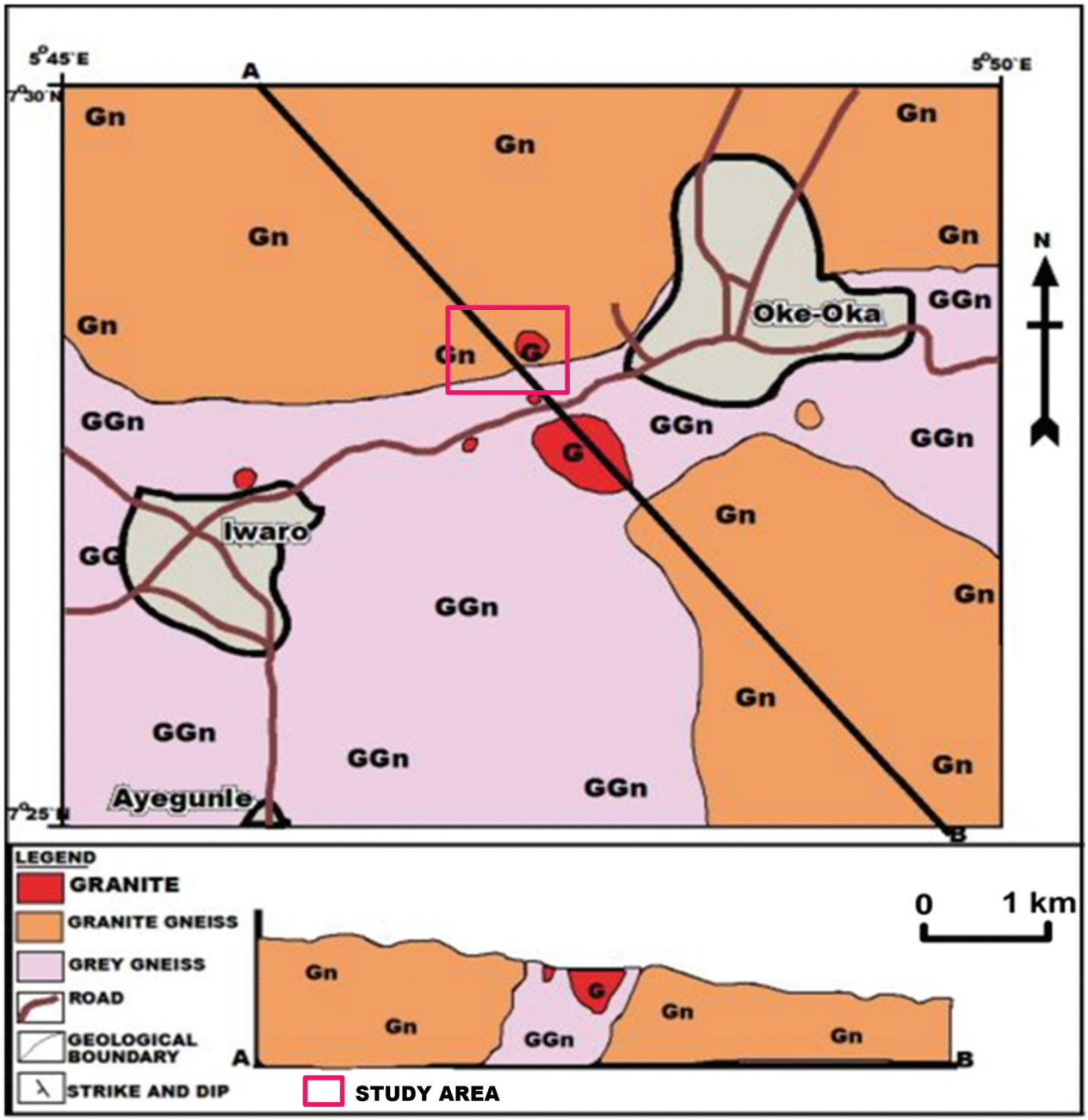

Figure 2. Geological map of the survey area.

The data were partially curve matched employing Zohdy (1965) technique and Orellana and Mooney (1966) using two-layer master curves and appropriate auxiliary charts as the first round investigation. This gives the resistivity and thickness of different subsurface layers at every VES station. The concluding phase of the interpretation was done with WinResist, an iteration modelling technique, where the model derived from the preliminary interpretation was inputted into the inversion algorithm (Vander Velper 2004). The values of resistivity and thickness obtained from the final model derived from the software were used to construct geoelectric sections (Figures 18b, 19b, 20b, 21b, 22, 23, 24, 25 and 26) along the various stations. The 2-D electrical resistivity imaging employed dipole–dipole array on selected four traverses to investigate lateral and vertical variations in conditions of the subsurface (Figure 3). Dipole spacing on the traverses was 10 m, and greater depth of penetration was attained by increasing the current dipole and potential dipole. The apparent resistivity values acquired were processed and inverted with the aid of DIPROfWIN 4.01 (Dipro for Windows 2001). This program computes an initial model and reduces the difference between the model and resistivity fields observed till a satisfactory fit is obtained. 2-D subsurface resistivity structures were interpreted with respect to subsurface lithology using the resistivity distribution, depending on the

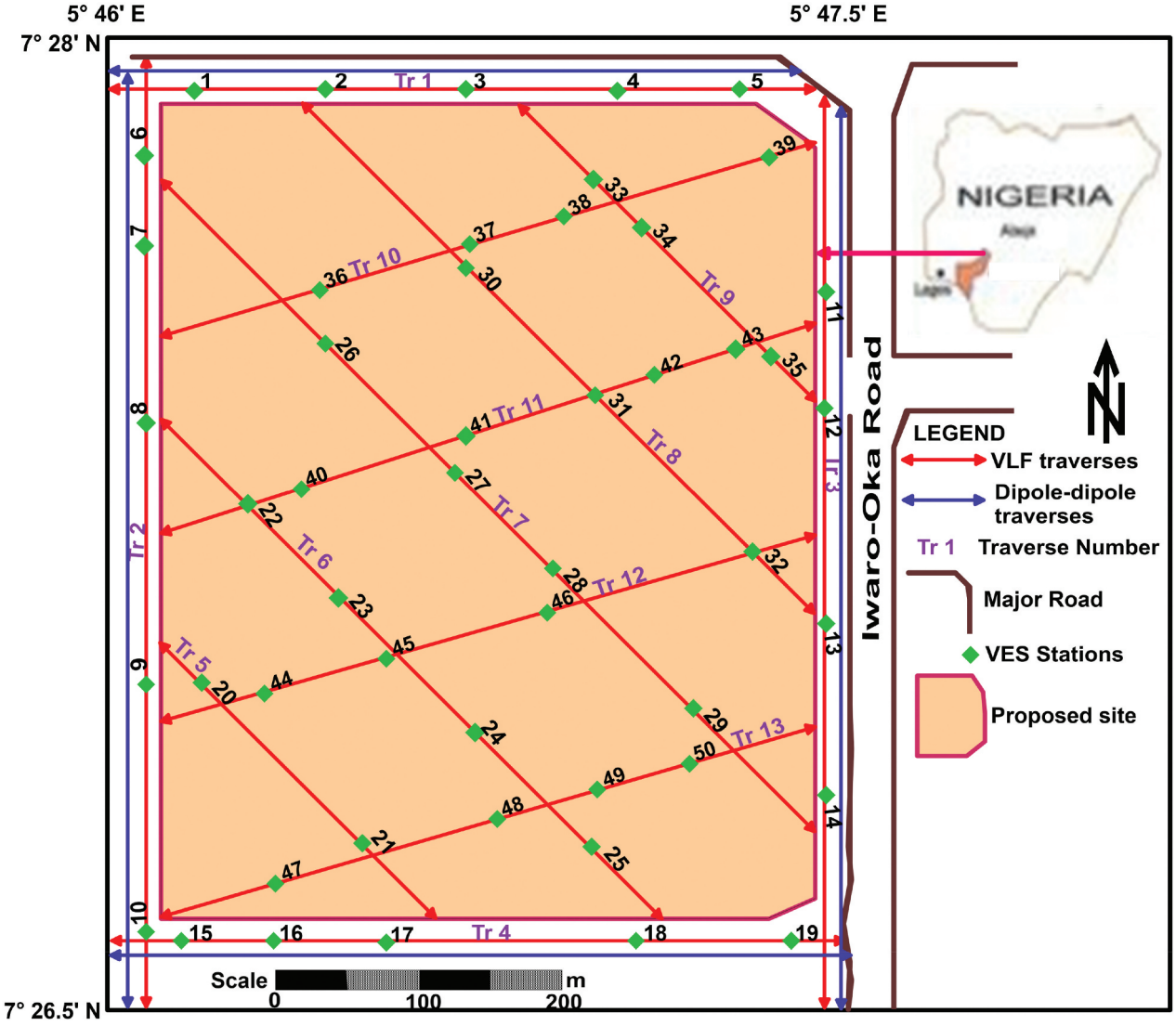

Figure 3. Geophysical data acquisition map of the survey area.

lateral and vertical continuity and geometry of the image responses as low continuous resistive subsurface substratum with resistivities ≤120 Ωm characterised by clay-rich material/water absorbing clayey layer/weathered basement, partially weathered/conductive fractured basement with resistivities between 130 and 950 Ωm and high laterally and/or vertically continuous resistivities (>1000 Ωm) interpreted as fresh bedrock.

4. Results and discussion

4.1. VLF–EM profiles and VLF–EM 2-D inverted models

The composite plots of the raw real and filtered real components against station positions as presented in Figures 4a–16a, enable qualitative identification of conductive zones in the subsurface. These positive peak anomalies of the VLF-EM profiles signify conductive zones and constitute the 50 vertical electrical sounding (VES) stations obtained along the 13 traverses across the study area (Figures 4a–16a). These conductive zones are indicative of faults/fractures, lithologic contacts, sheared zones, basement depression, weathered basement and other weak zones that enhance accumulation of water and form pathways for groundwater, and are disastrous to structural foundation of civil earth works. The Karous-Hjelt 2D inverted models give the pictorial distribution of conductive geologic features relative to depth (Figures 4b–16b). Varying conductive subsurface materials (green to red) were recognised trending differently across the sections.

4.1.1. Traverse 1

Conductive subsurface features were identified at distance of 75, 170, 255, 365 and 410 m along traverse 1 (Figure 4a). These features indicate conductive fractured zones. These zones although are significant in groundwater development but act as weak zones that could pose significant threat to

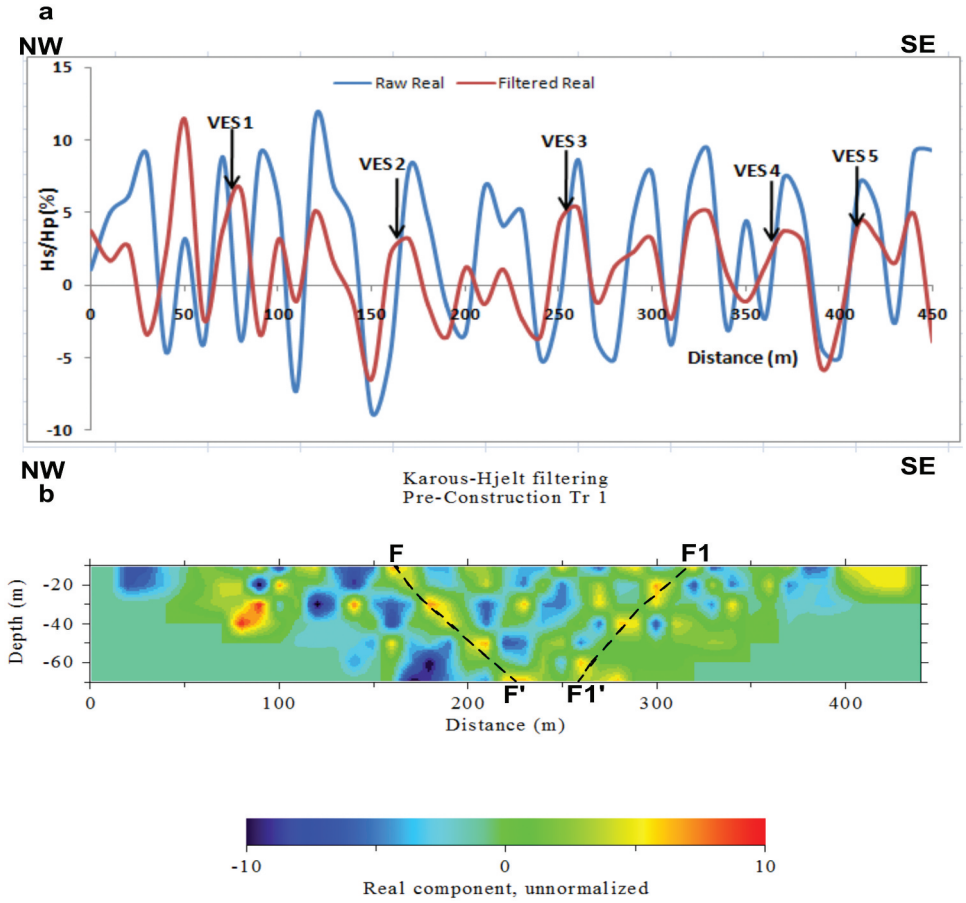

Figure 4. (a) VLF-EM plot of real components and (b) corresponding 2-D inverted section of Traverse 1.

structural foundation of the proposed construction works in the study area. The 2-D inversion model showed cross-cutting conductive bodies at distance between 50–120 m, 200–370 m and 390–440 m on the VLF-EM section (Figure 4b). They are weak zones within the subsurface which could facilitate failure/total collapse of the proposed civil construction works if necessary measures are not put in place to mitigate possible challenges. Conductive zones at distance between 165–225 m (F–F') and 260–320 m (F1–F1′) (Figure 4b) are typical linear features (fractures) coincide with the weak zones on the VLF-EM profile (Figure 4a).

4.1.2. Traverse 2

Conductive points at distance 80, 118, 270, 470 and 555 m along traverse 2 (Figure 5a) suggest geologic structures such as faults, fractures, depression and geologic contacts which are indicative of incompetent layer across the area. Similarly, at 20–170, 260–300 and 410–480 m are major high conductive zones trending in different directions across the section (Figure 5b). Conductive structures at different points indicate incompetent engineering zones within the area. Observations of conductive structures on this profile correlate with the weak zones on the 2-D inverted model. The conductive subsurface structures between distance 45–160 (F2–F2′), 260–300 (F3–F3′) and 410–475 m (F4–F4′) are indicative of incompetent geologic formation which could lead to instability of structural foundation.

4.1.3. Traverse 3

Conductive bodies at distance 170, 240, 367 and 480 m along traverse 3 (Figure 6a) indicate faults, fractures, depressions, clay and geologic contacts which are unsuitable for building construction. The 2-D inverted model identified several oval shapes of high conductive bodies across the area which suggest pocket of clay materials between station distance 100–250 and 300–520 m (Figure 6b). Identified conductive features on the profile relate to that on 2-D inverted model. The observed linear conductive features between distance 180–250 (F5–F5′) and 300–370 m (F6–F6′) signify incompetent geologic unit with potential subsurface structural foundation problem (Figure 6b).

4.1.4. Traverse 4

Conductive structures at distance 60, 145, 200, 355 and 410 m along traverse 4 (Figure 7a) signify basement depression or fractured zones. These conductive zones accumulate groundwater and serve as pathway for groundwater, thus constitute weak

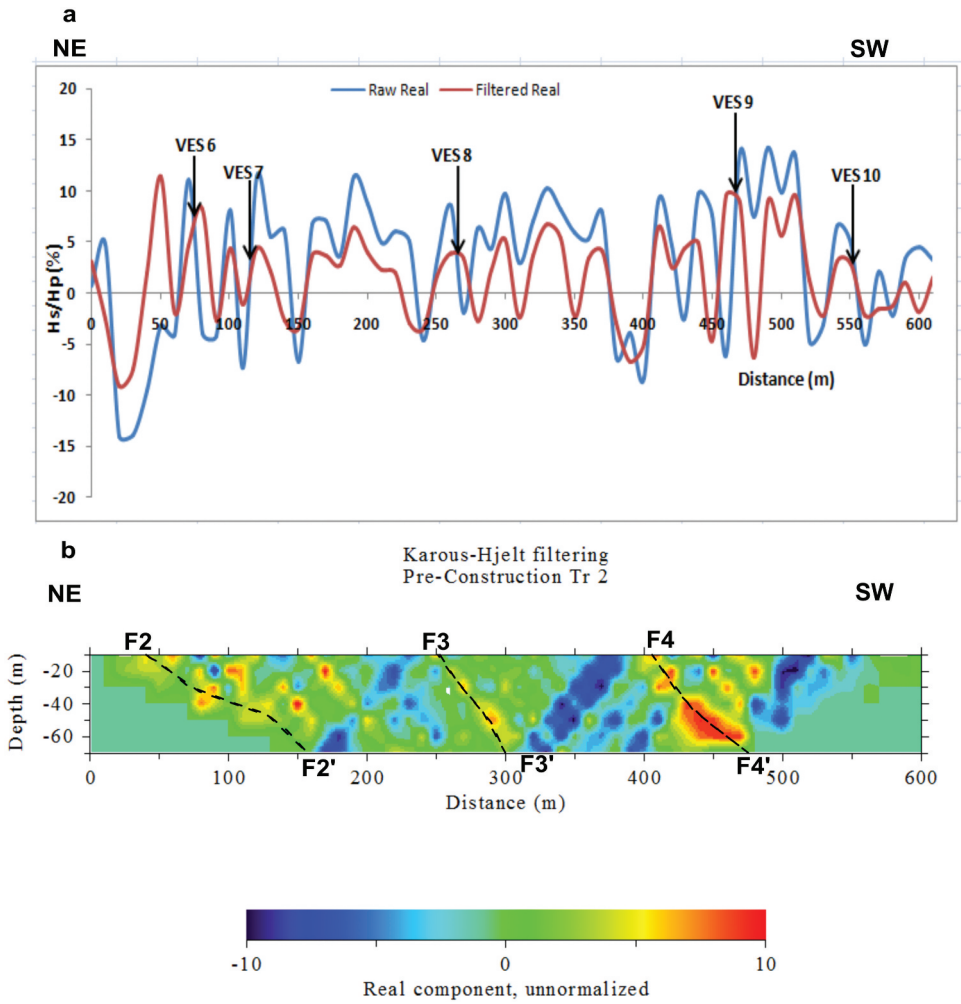

Figure 5. (a) VLF-EM plot of real components and (b) corresponding 2-D inverted section of Traverse 2.

zones that threaten stability of construction works if constructed on it. The 2-D model is characterised by conductive features at distances 50–180 m, 200–360 m and 400–440 m dipping NW–SE and NE–SW (Figure 7b). The observed pockets of clay materials are indicative of weak/incompetent geologic formation underlying the location that can precipitate failure of the proposed building if not considered during foundation design and construction. Typical linear conductive feature (fracture, F7–F7′) is identified at point 140–175 m that could adversely impact the foundation of proposed construction works (Figure 7b).

4.1.5. Traverses 5 and 6

The VLF-EM profiles revealed conductive features at distance 25 and 190 along traverse 5 (Figure 8a) and 70, 130, 250 and 380 m along traverse 6 (Figure 9a) indicative of the presence of fracture. These conductive features on the profiles correspond to the observable conductive anomaly on the 2-D inverted models at the distance between 30–65 m and 85–220 m (Figure 8b) and 60–130 and 200–425 m (Figure 9b). It also shows resistive features, which may be due to closeness of outcrop to the location. The inverted sections in the survey area depict an uneven subsurface topography reflecting different degree of conductivities. The observed conductive linear features at these locations suggest the likelihood of conductive materials at depth, indicative of the presence of fractures and basement depressions constituting water collection zones and saturated clay which are unsuitable to support massive and multistorey building projects. The Identified conductive features on the profiles relate to conductive zones established in 2-D inverted models. The fractured zones (F8–F8′ and F9–F9′) are engineering incompetent zones that could pose significant threat to structural foundation of the proposed construction works in the study area (Figures 8b and 9b), thus needed to be considered during foundation design and adequately addressed during construction for safe and sustainable structures.

4.1.6. Traverses 7, 8 and 9

The points of inflection of the raw real coincide with the positive peak of the filtered real at distance 125, 250, 310 and 490 m along traverse 7 (Figure 10a), 118, 245 and 405 m along traverse 8 (Figure 11a) and 70, 125 and 230 m along traverse 9 (Figure 12a). These positive

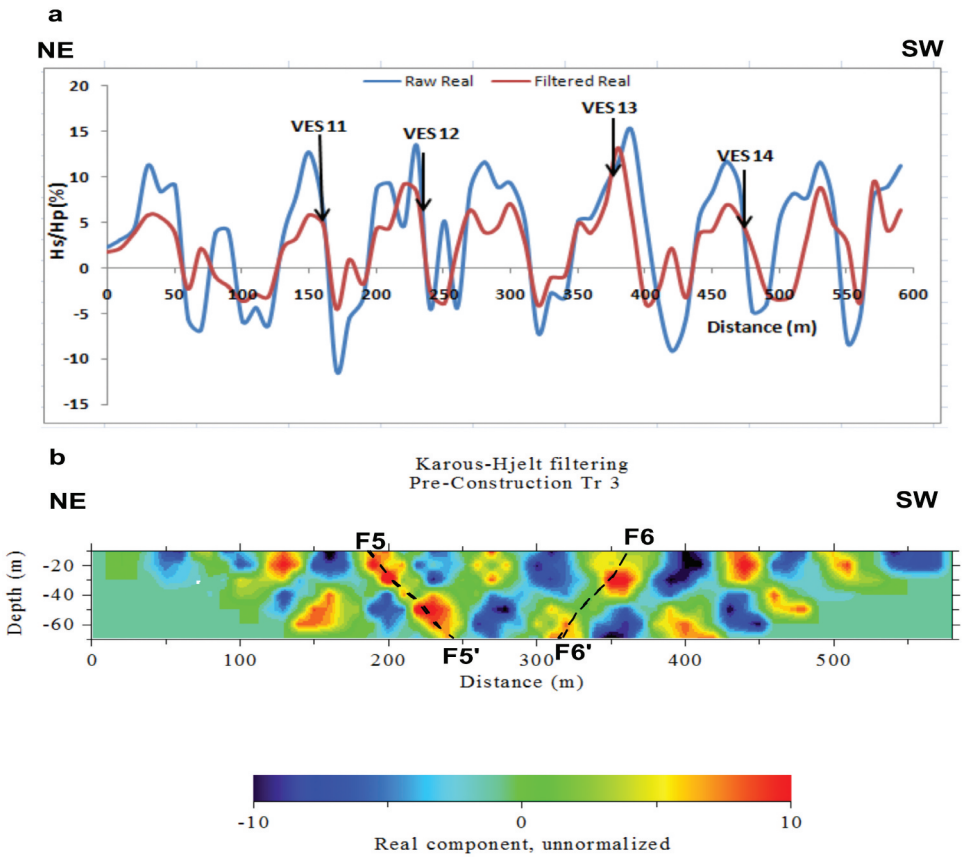

Figure 6. (a) VLF-EM plot of real components and (b) corresponding 2-D inverted section of Traverse 3.

peaks are indicative of the presence of conductive zones; clayey layers, basement depression, faults or fractured zones. These conductive zones accumulate groundwater and serve as pathway for groundwater, thus constitute weak zones that threaten stability of construction works if constructed on it. The 2-D inverted models reveal points showing major conductive features of varying degree of conductivity trending in different directions on the sections. The observations of the conductive features on the VLF-EM profiles correspond with the incompetent zones on the 2-D sections at 20–130, 200–400 and 460–590 m along traverse 7 (Figure 10b), 70–130, 160–320 and 380–420 m along traverse 8 (Figure 11b) and 10–30, 60–135 and 190–260 m along traverse 9 (Figure 12b). These conductive zones are relevant in groundwater exploitation but disastrous to structural development. Fracture zones; F10–F10′, F11–F11′ and F12–F12′–F12" in Figures 10b, 11b and 12b respectively are weak zones constituting rock instability and if not properly addressed during construction could adversely impact the foundation of the construction works. The identified fractured zones on the VLF-EM 2-D inverted models correspond to the identified conductive features on the profiles, and they are engineering incompetent formation which could result in differential foundation movement causing wall cracks and collapse of buildings.

4.1.7. Traverses 10, 11, 12 and 13

Conductive bodies identified on the EM profiles at 125, 250, 320 and 430 m along traverse 10 (Figure 13a), 75, 185, 305 and 370 m along traverse 11 (Figure 14a), 70, 125 and 250 m along traverse 12 (Figure 15a) and 65, 245, 295 and 355 m along traverse 13 (Figure 16a) suggest conductive subsurface geologic structures such as faults, fractures, basement depressions, lithologic contacts and even clay materials which are incompetent geotechnical layer across the area unsuitable for siting civil engineering structures in a typical basement complex terrain. Similarly, the 2-D inverted models identified conductive linear structures between distances 20–40, 70–130, 190–300 and 330–430 m along traverse 10 (Figure 13b), 30–200 and 250–390 m along traverse 11 (Figure 14b), 10–30, 65–130 and 180–350 m along traverse 12 (Figure 15b), 15–50, 70–170 and 190–400 m along traverse 13 (Figure 16b). The presence of these high conductive zones trending in different directions across the survey area indicates engineering subsurface incompetent layers across the area. Observations of the conductive features on the EM profiles correlate with the established conductive zones on 2-D inverted models. Also, the existence of prominent near surface linear conductive zones, fractures between distance 220–300 (F13–F13′), 100–190 (F14–F14′), 220–285 (F15–F15′) and 185–310 m (F16–F16′) (Figures 13b, 14b, 15b and 16b respectively) serve

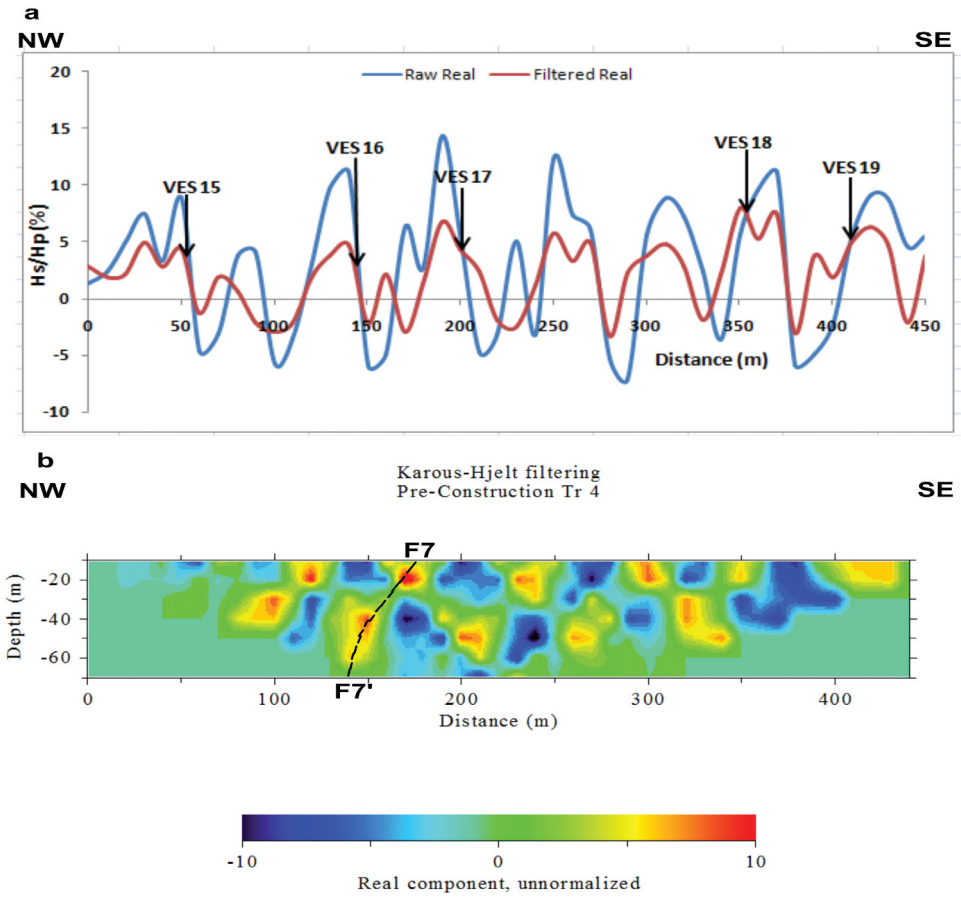

Figure 7. (a) VLF-EM plot of real components and (b) corresponding 2-D inverted section of Traverse 4.

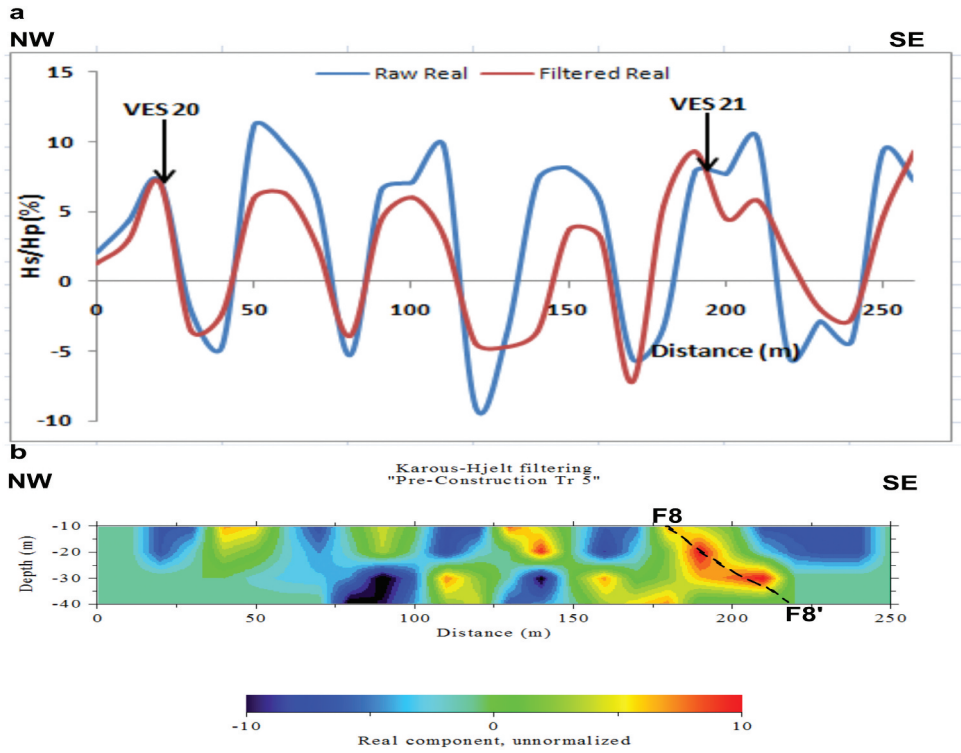

Figure 8. (a) VLF-EM plot of real components and (b) corresponding 2-D inverted section of Traverse 5.

as subsurface conduits for migration and accumulation of groundwater, unfavourable to construction projects as they permit interaction of subsoil with water resulting in reduction of its load bearing capacity.

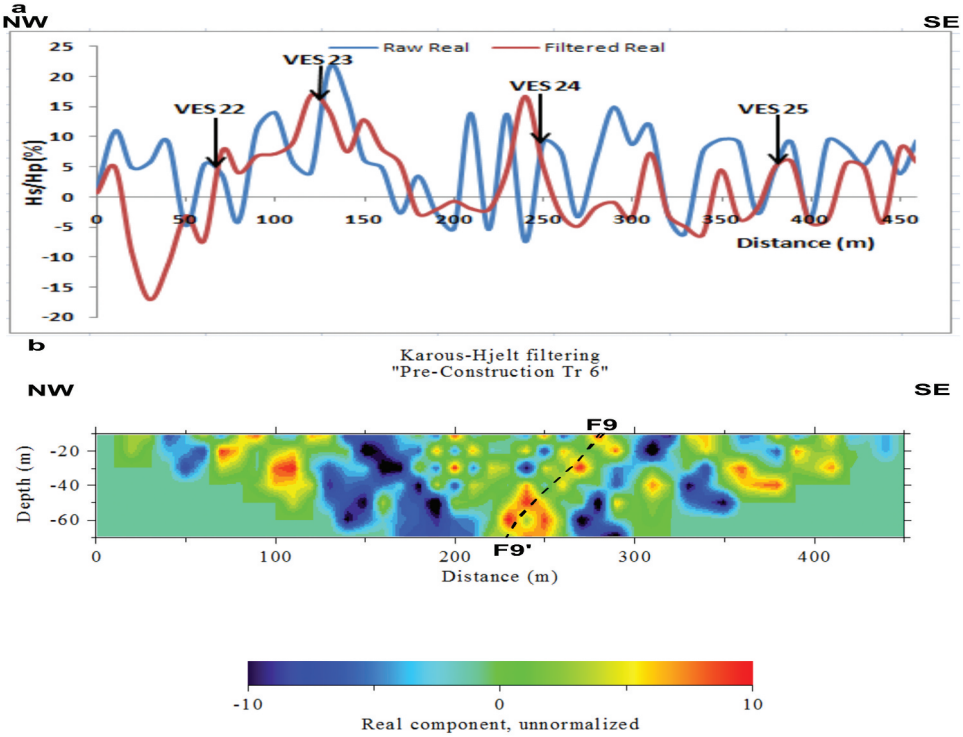

Figure 9. (a) VLF-EM plot of real components and (b) corresponding 2-D inverted section of Traverse 6.

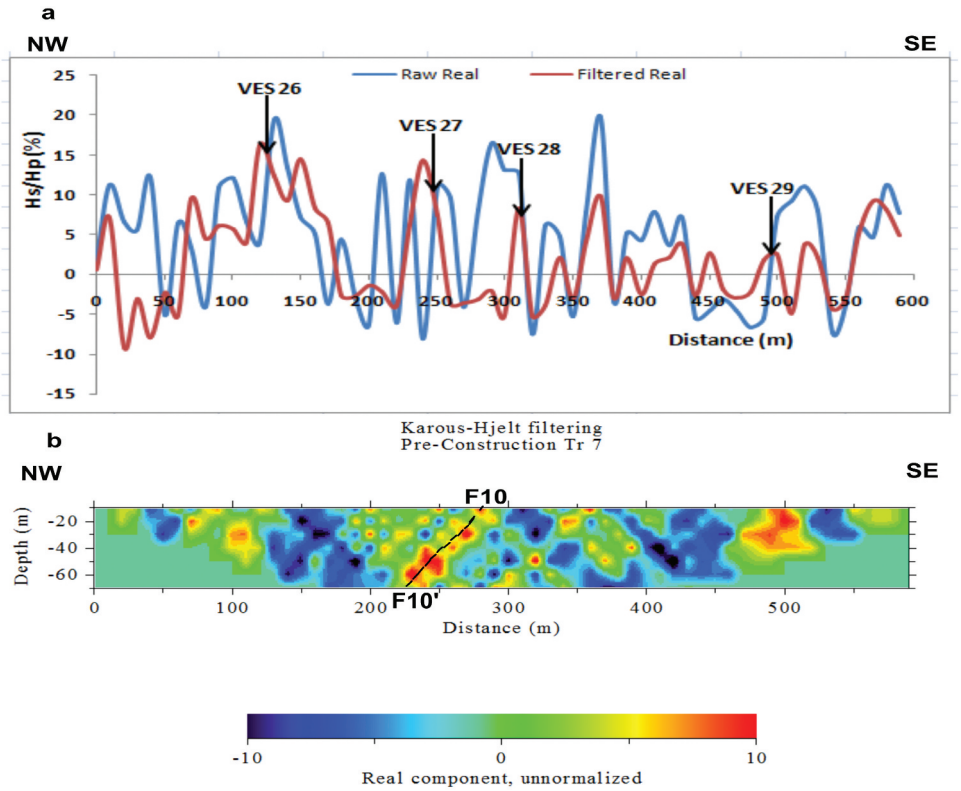

Figure 10. (a) VLF-EM plot of real components and (b) corresponding 2-D inverted section along Traverse 7.

4.2. Electrical resistivity results

The 50 VES stations investigated from the VLF-EM survey are displayed as sounding curves, tables, geoelectric sections and maps. The quantitative interpretation of the sounding curves provides geoelectric parameters used to generate the geoelectric sections (Figures 18b, 19b, 20b, 21b, 22, 23, 24, 25 and 26). The geoelectric sections represent the geologic sequence mapped with respect to depth. The 2-D subsurface resistivity structures were interpreted with respect to subsurface lithology using the resistivity distribution, depending on lateral and vertical continuity and

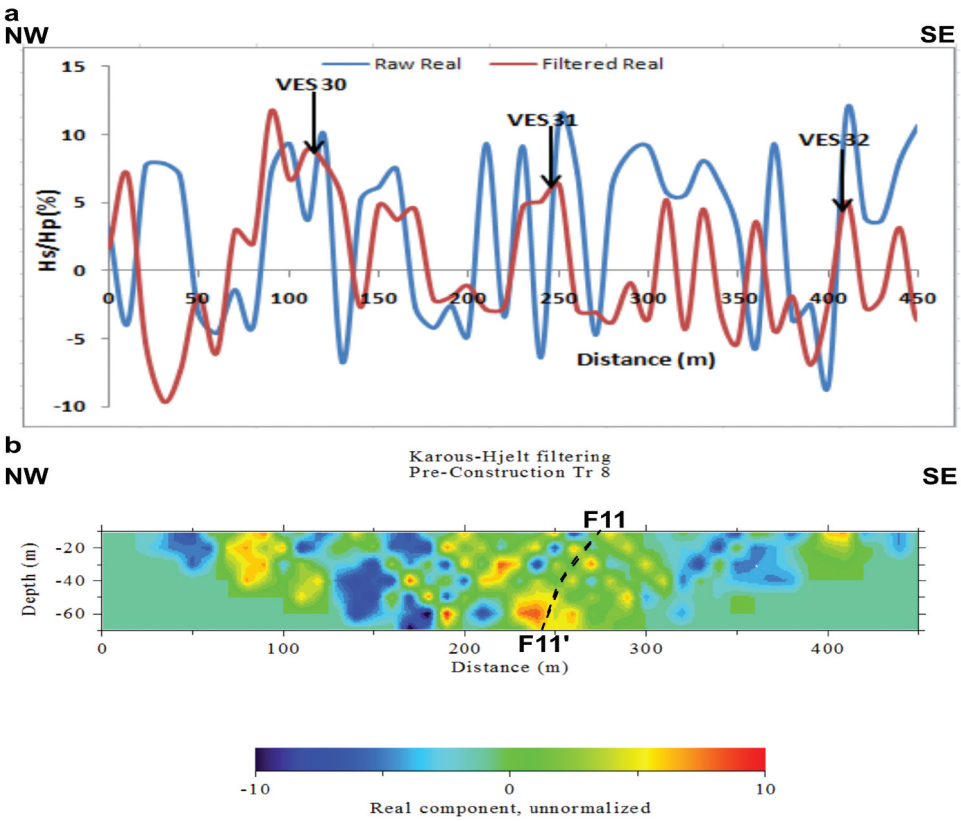

Figure 11. (a) VLF-EM plot of real components and (b) corresponding 2-D inverted section along Traverse 8.

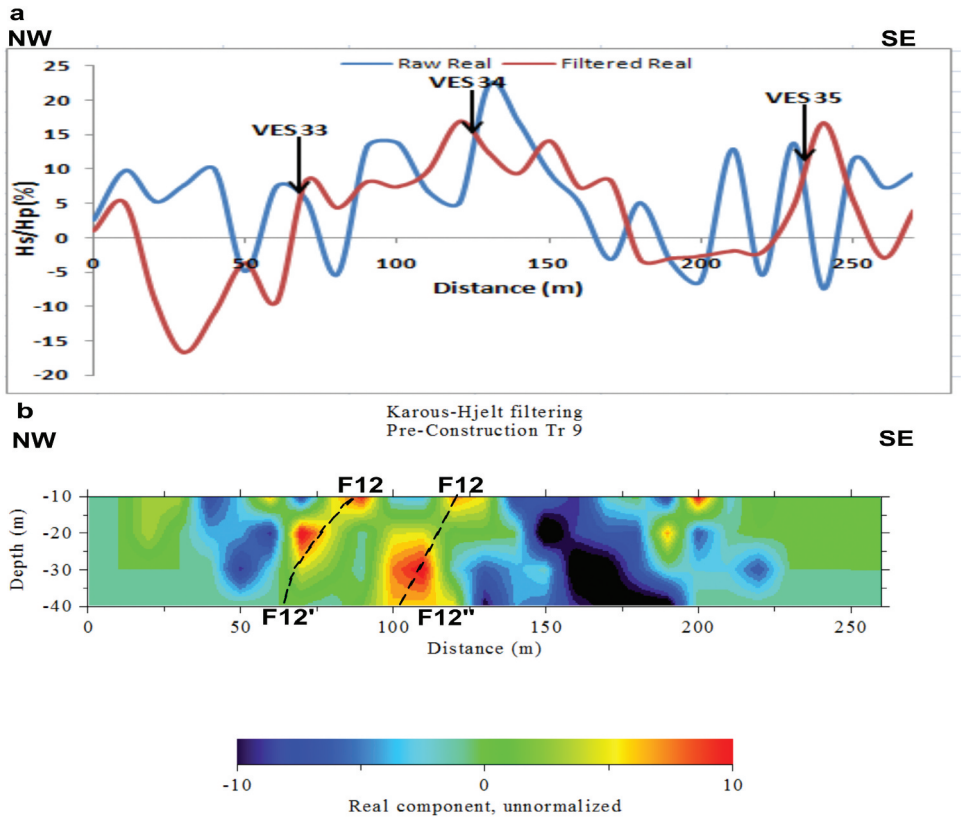

Figure 12. (a) VLF-EM plot of real components and (b) corresponding 2-D inverted section along Traverse 9.

geometry of the image responses and interpreted in terms of subsurface lithology. Results from the electrical resistivity method revealed the pattern of resistivity variations within the study area with insight into the geoelectric characteristics of the geologic units giving the engineering competency/suitability of each

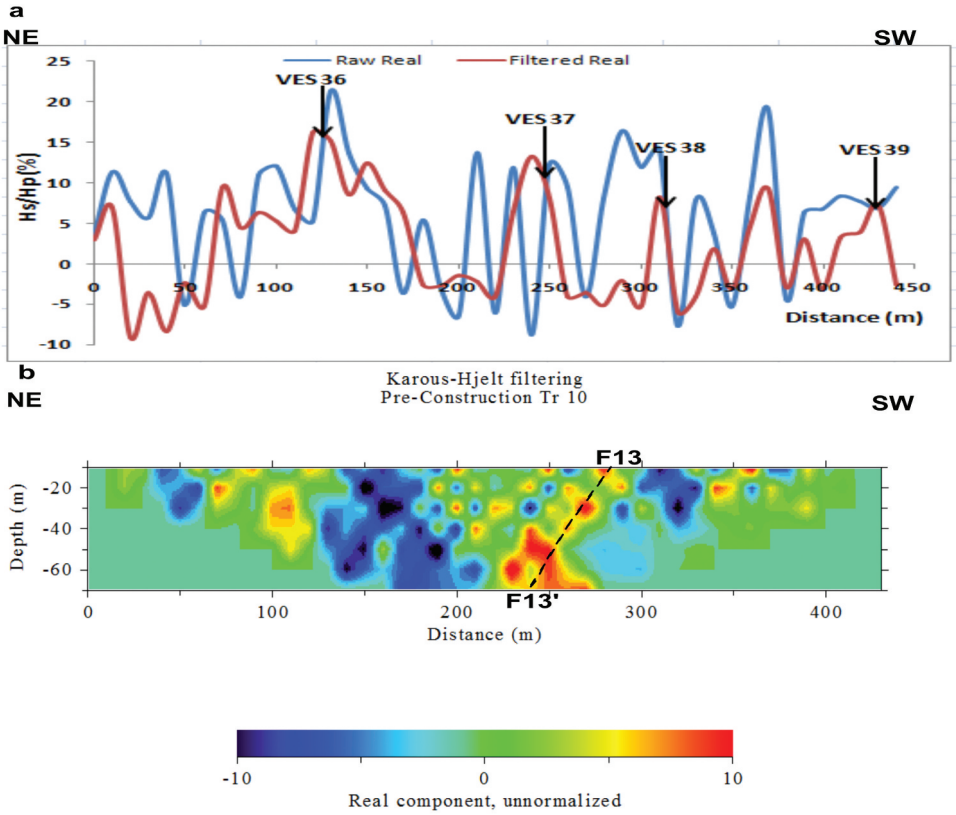

Figure 13. (a) VLF-EM plot of real components and (b) corresponding 2-D inverted section of Traverse 10.

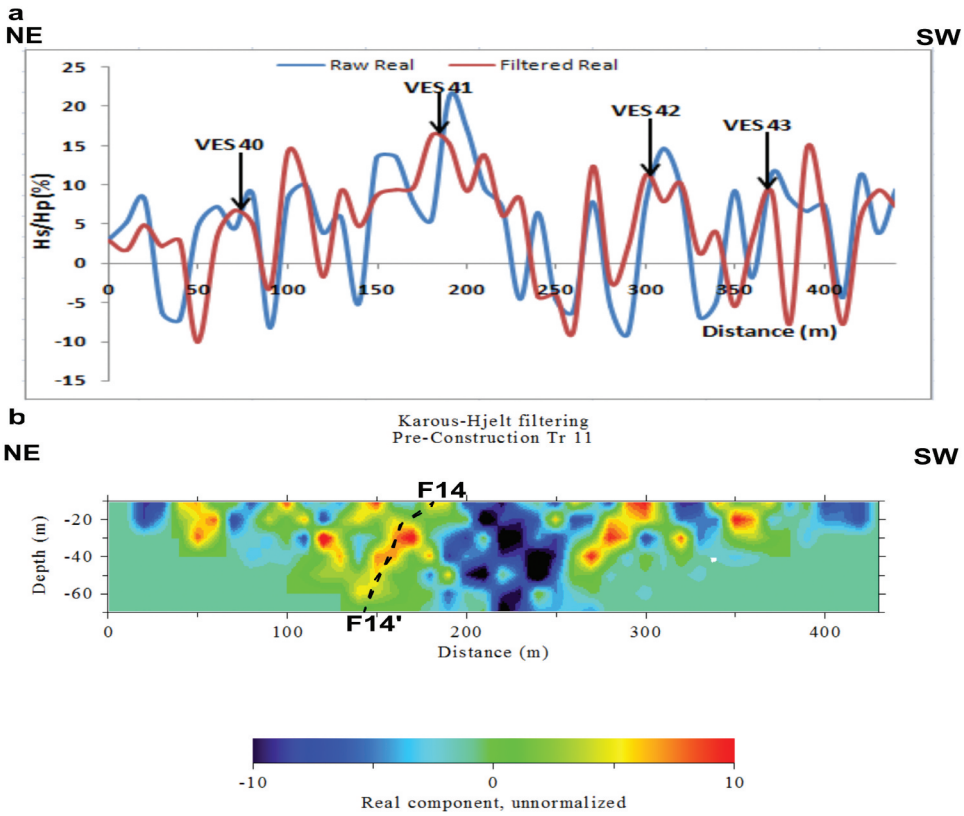

Figure 14. (a) VLF-EM plot of real components and (b) corresponding 2-D inverted section of Traverse 11.

layer with depth. Two curve types are identified from the site: HA and AA curve types (Table 1 and Figure 17). The curve types represent four distinctive lithologic layers: topsoil (top layer), weathered basement, partially weathered/fractured bedrock and fresh basement (Table 1). The HA-curve type dominates the

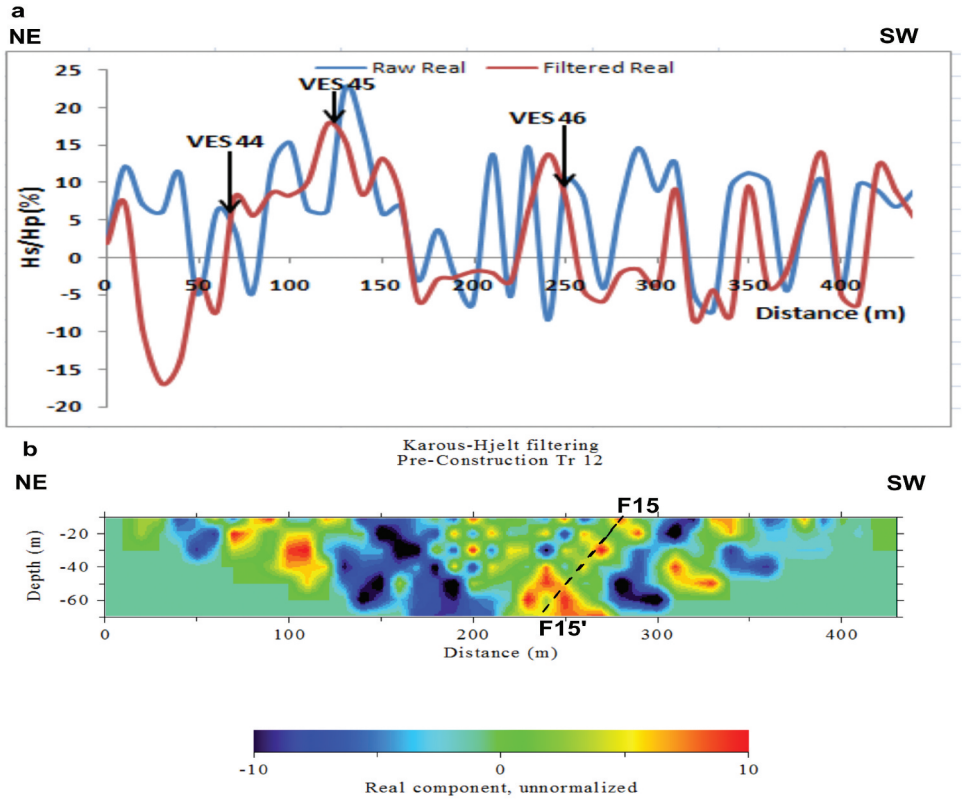

Figure 15. (a) VLF-EM plot of real components and (b) corresponding 2-D inverted section of Traverse 12.

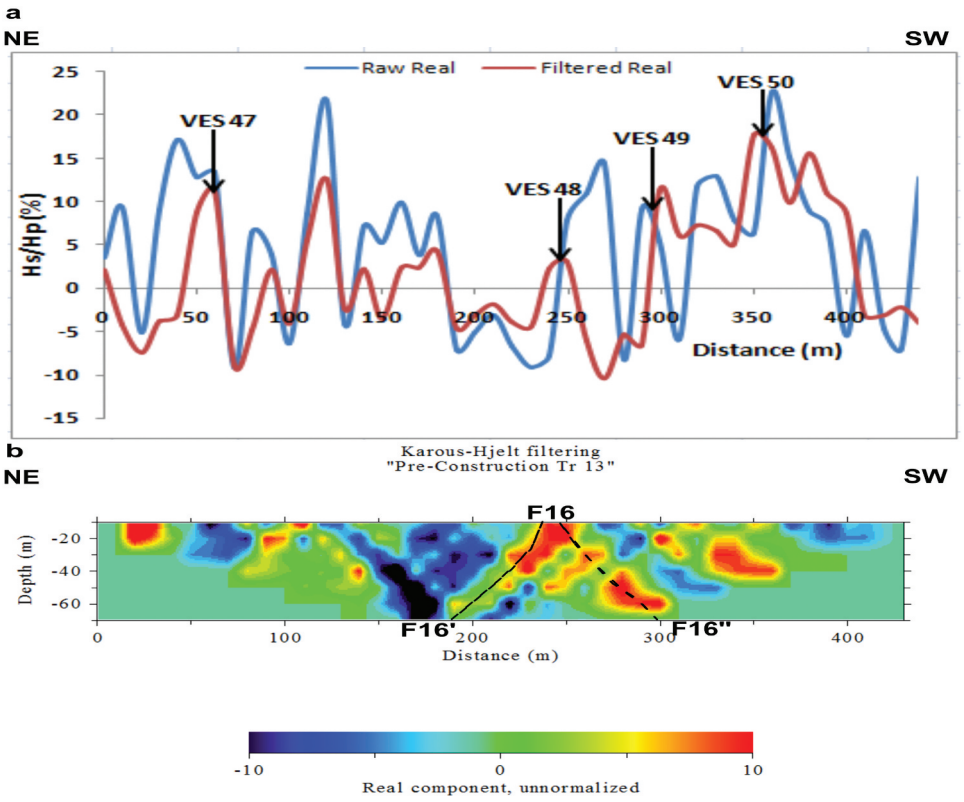

Figure 16. (a) VLF-EM plot of real components and (b) corresponding 2-D inverted section of Traverse 13.

study area with a percentage frequency of 82%, while AA-curve type has 18% of occurrence. The inverted subsurface 2-D resistivity structures along the four traverses are characterised by three different resistivity responses: low resistivity response (generally <120 Ohm-m), intermediate resistivity

Table 1. Interpretation of the VES curves and corresponding lithology.

VES Number	Layer	Resistivity (Ohm-m)	Thickness (m)	Depth (m)	Lithology	VES curve
1	1	238	1.4	1.4	Topsoil	HA
	2	47	5.5	6.9	Weathered basement (clay)	
	3	280	8.2	15.1	Fractured/Partially weathered bedrock (sand)	
	4	1343	-	-	Fresh basement	
2	1	279	1.2	1.2	Topsoil	HA
	2	56	7.4	8.6	Weathered basement (clay)	
	3	345	9.9	18.5	Fractured/Partially weathered bedrock (sand)	
	4	1338	-	-	Fresh basement	
3	1	350	1.3	1.3	Topsoil	HA
	2	48	5.5	6.9	Weathered basement (clay)	
	3	261	9.2	16.0	Fractured/Partially weathered bedrock (sand)	
	4	1052	-	-	Fresh basement	
4	1	272	1.1	1.1	Topsoil	HA
	2	48	5.0	6.1	Weathered basement (clay)	
	3	371	8.4	14.5	Fractured/Partially weathered bedrock (sand)	
	4	1609	-	-	Fresh basement	
5	1	327	1.4	1.4	Topsoil	HA
	2	50	4.6	6.0	Weathered basement (clay)	
	3	467	7.6	13.6	Fractured/Partially weathered bedrock (sand)	
	4	1618	-	-	Fresh basement	
6	1	324	1.4	1.4	Topsoil	HA
	2	61	5.1	6.5	Weathered basement (clay)	
	3	381	9.2	15.7	Fractured/Partially weathered bedrock (sand)	
	4	1272	-	-	Fresh basement	
7	1	296	1.4	1.4	Topsoil	HA
	2	57	5.3	6.7	Weathered basement (clay)	
	3	346	12.6	19.2	Fractured/Partially weathered bedrock (sand)	
	4	1123	-	-	Fresh basement	
8	1	171	1.6	1.6	Topsoil	HA
	2	54	4.5	6.0	Weathered basement (clay)	
	3	375	9.1	15.1	Fractured/Partially weathered bedrock (sand)	
	4	1296	-	-	Fresh basement	
9	1	329	1.5	1.5	Topsoil	HA
	2	69	5.1	6.5	Weathered basement (clay)	
	3	402	9.8	16.4	Fractured/Partially weathered bedrock (sand)	
	4	1244	-	-	Fresh basement	
10	1	178	2.0	2.0	Topsoil	HA
	2	43	6.2	8.3	Weathered basement (clay)	
	3	378	9.4	17.7	Fractured/Partially weathered bedrock (sand)	
	4	2195	-	-	Fresh basement	
11	1	119	1.1	1.1	Topsoil	HA
	2	59	3.1	4.3	Weathered basement (clay)	
	3	589	8.0	12.3	Fractured/Partially weathered bedrock (sand)	
	4	1204	-	-	Fresh basement	
12	1	217	0.7	0.7	Topsoil	HA
	2	69	14.6	15.4	Weathered basement (clay)	
	3	195	11.5	26.8	Fractured/Partially weathered bedrock (sandy clay)	
	4	1963	-	-	Fresh basement	
13	1	357	1.5	1.5	Topsoil	HA
	2	72	6.6	8.1	Weathered basement (clay)	
	3	339	10.4	18.5	Fractured/Partially weathered bedrock (sand)	
	4	947	-	-	Fresh basement	
14	1	97	1.7	1.7	Topsoil	AA
	2	129	5.5	7.2	Weathered basement (clay)	
	3	191	10.4	17.6	Fractured/Partially weathered bedrock (sandy clay)	
	4	2217	-	-	Fresh basement	
15	1	247	1.9	1.9	Topsoil	HA
	2	76	4.5	6.4	Weathered basement (clay)	
	3	467	8.8	15.2	Fractured/Partially weathered bedrock (sand)	
	4	1252	-	-	Fresh basement	
16	1	461	1.8	1.8	Topsoil	HA
	2	50	5.2	7.1	Weathered basement (clay)	
	3	399	6.8	13.6	Fractured/Partially weathered bedrock (sand)	
	4	1494	-	-	Fresh basement	
17	1	183	1.3	1.3	Topsoil	HA
	2	60	4.2	5.5	Weathered basement (clay)	
	3	437	9.0	14.5	Fractured/Partially weathered bedrock (sand)	
	4	1163	-	-	Fresh basement	
18	1	34	1.3	1.3	Topsoil	AA
	2	153	12.6	13.9	Weathered basement (sandy clay)	
	3	301	11.0	24.8	Fractured/Partially weathered bedrock (sand)	
	4	1609	-	-	Fresh basement	
19	1	91	6.8	6.8	Topsoil	AA
	2	140	7.5	14.3	Weathered basement (sandy clay)	
	3	408	8.8	23.0	Fractured/Partially weathered bedrock (sand)	
	4	1440	-	-	Fresh basement	

(*Continued*)

Table 1. (Continued).

VES Number	Layer	Resistivity (Ohm-m)	Thickness (m)	Depth (m)	Lithology	VES curve
20	1	130	8.1	8.1	Topsoil	HA
	2	57	9.3	17.4	Weathered basement (clay)	
	3	368	8.8	26.2	Fractured/Partially weathered bedrock (sand)	
	4	1969	-	-	Fresh basement	
21	1	127	9.5	9.5	Topsoil	HA
	2	89	12.3	21.8	Weathered basement (clay)	
	3	360	10.0	31.7	Fractured/Partially weathered bedrock (sand)	
	4	1329	-	-	Fresh basement	
22	1	98	8.7	8.7	Topsoil	AA
	2	148	7.8	16.5	Weathered basement (sandy clay)	
	3	426	9.3	25.8	Fractured/Partially weathered bedrock (sand)	
	4	1627	-	-	Fresh basement	
23	1	77	4.5	4.5	Topsoil	AA
	2	175	5.2	9.6	Weathered basement (sandy clay)	
	3	507	8.0	17.6	Fractured/Partially weathered bedrock (sand)	
	4	1881	-	-	Fresh basement	
24	1	307	0.8	0.8	Topsoil	HA
	2	51	3.4	4.2	Weathered basement (clay)	
	3	510	7.6	11.8	Fractured/Partially weathered bedrock (sand)	
	4	1839	-	-	Fresh basement	
25	1	136	2.3	2.3	Topsoil	HA
	2	62	4.4	6.8	Weathered basement (clay)	
	3	425	8.8	15.6	Fractured/Partially weathered bedrock (sand)	
	4	1424	-	-	Fresh basement	
26	1	507	0.8	0.8	Topsoil	HA
	2	70	3.9	4.7	Weathered basement (clay)	
	3	443	11.4	16.2	Fractured/Partially weathered bedrock (sand)	
	4	1052	-	-	Fresh basement	
27	1	183	0.9	0.9	Topsoil	HA
	2	54	2.6	3.5	Weathered basement (clay)	
	3	629	6.9	10.4	Fractured/Partially weathered bedrock (sand)	
	4	1353	-	-	Fresh basement	
28	1	255	1.5	1.5	Topsoil	HA
	2	68	4.9	6.4	Weathered basement (clay)	
	3	483	7.8	14.2	Fractured/Partially weathered bedrock (sand)	
	4	1610	-	-	Fresh basement	
29	1	274	1.6	1.6	Topsoil	HA
	2	70	6.4	8.0	Weathered basement (clay)	
	3	400	10.0	18.0	Fractured/Partially weathered bedrock (sand)	
	4	1145	-	-	Fresh basement	
30	1	180	1.3	1.3	Topsoil	HA
	2	67	3.1	4.4	Weathered basement (clay)	
	3	524	7.3	11.7	Fractured/Partially weathered bedrock (sand)	
	4	1068	-	-	Fresh basement	
31	1	170	1.6	1.6	Topsoil	HA
	2	62	3.8	5.4	Weathered basement (clay)	
	3	436	8.1	13.6	Fractured/Partially weathered bedrock (sand)	
	4	1212	-	-	Fresh basement	
32	1	34	4.7	4.7	Topsoil	AA
	2	104	3.1	7.8	Weathered basement (sandy clay)	
	3	362	4.6	12.4	Fractured/Partially weathered bedrock (sand)	
	4	4105	-	-	Fresh basement	
33	1	276	2.3	2.3	Topsoil	HA
	2	69	7.2	9.5	Weathered basement (clay)	
	3	321	7.9	17.4	Fractured/Partially weathered bedrock (sand)	
	4	1714	-	-	Fresh basement	
34	1	90	3.0	3.0	Topsoil	AA
	2	143	4.4	7.4	Weathered basement (sandy clay)	
	3	461	6.1	13.6	Fractured/Partially weathered bedrock (sand)	
	4	2561	-	-	Fresh basement	
35	1	326	0.6	0.6	Topsoil	HA
	2	66	2.6	3.1	Weathered basement (clay)	
	3	305	14.9	18.1	Fractured/Partially weathered bedrock (sand)	
	4	1943	-	-	Fresh basement	
36	1	165	1.4	1.4	Topsoil	HA
	2	66	4.0	5.4	Weathered basement (clay)	
	3	559	8.6	14.0	Fractured/Partially weathered bedrock (sand)	
	4	1440	-	-	Fresh basement	
37	1	27	6.0	6.0	Topsoil	AA
	2	101	8.6	14.6	Weathered basement (clay)	
	3	269	9.3	23.9	Fractured/Partially weathered bedrock (sand)	
	4	1503	-	-	Fresh basement	
38	1	466	1.5	1.5	Topsoil	HA
	2	69	5.1	6.6	Weathered basement (clay)	
	3	428	9.7	16.3	Fractured/Partially weathered bedrock (sand)	
	4	1258	-	-	Fresh basement	

(*Continued*)

Table 1. (Continued).

VES Number	Layer	Resistivity (Ohm-m)	Thickness (m)	Depth (m)	Lithology	VES curve
39	1	373	1.5	1.5	Topsoil	HA
	2	67	9.2	10.8	Weathered basement (clay)	
	3	325	11.4	22.1	Fractured/Partially weathered bedrock (sand)	
	4	1246	-	-	Fresh basement	
40	1	182	3.8	3.8	Topsoil	HA
	2	70	9.5	13.3	Weathered basement (clay)	
	3	324	11.0	24.3	Fractured/Partially weathered bedrock (sand)	
	4	1380	-	-	Fresh basement	
41	1	57	2.0	2.0	Topsoil	AA
	2	130	6.1	8.1	Weathered basement (sandy clay)	
	3	512	8.0	16.1	Fractured/Partially weathered bedrock (sand)	
	4	2110	-	-	Fresh basement	
42	1	353	1.4	1.4	Topsoil	HA
	2	56	5.7	7.2	Weathered basement (clay)	
	3	333	8.0	15.2	Fractured/Partially weathered bedrock (sand)	
	4	1689	-	-	Fresh basement	
43	1	262	2.1	2.1	Topsoil	HA
	2	30	5.6	7.7	Weathered basement (clay)	
	3	536	9.8	17.5	Fractured/Partially weathered bedrock (sand)	
	4	3229	-	-	Fresh basement	
44	1	236	2.5	2.5	Topsoil	HA
	2	34	9.8	12.3	Weathered basement (clay)	
	3	331	10.6	22.9	Fractured/Partially weathered bedrock (sand)	
	4	1600	-	-	Fresh basement	
45	1	456	1.7	1.7	Topsoil	HA
	2	61	6.1	7.8	Weathered basement (clay)	
	3	330	8.8	16.6	Fractured/Partially weathered bedrock (sand)	
	4	1996	-	-	Fresh basement	
46	1	219	1.2	1.2	Topsoil	HA
	2	21	4.0	5.1	Weathered basement (clay)	
	3	451	7.3	12.5	Fractured/Partially weathered bedrock (sand)	
	4	1627	-	-	Fresh basement	
47	1	402	2.0	2.0	Topsoil	HA
	2	46	4.1	6.1	Weathered basement (clay)	
	3	495	6.2	12.1	Fractured/Partially weathered bedrock (sand)	
	4	2682	-	-	Fresh basement	
48	1	331	1.5	1.5	Topsoil	HA
	2	73	6.2	7.7	Weathered basement (clay)	
	3	359	9.8	17.6	Fractured/Partially weathered bedrock (sand)	
	4	1272	-	-	Fresh basement	
49	1	301	2.2	2.2	Topsoil	HA
	2	33	4.8	7.0	Weathered basement (clay)	
	3	432	6.8	13.8	Fractured/Partially weathered bedrock (sand)	
	4	3923	-	-	Fresh basement	
50	1	314	1.5	1.5	Topsoil	HA
	2	58	5.2	6.6	Weathered basement (clay)	
	3	397	9.3	16.0	Fractured/Partially weathered bedrock (sand)	
	4	1388	-	-	Fresh basement	

responses (resistivity in the range 130–575 Ohm-m) and high resistivity responses having resistivity above 1000 Ohm-m.

4.2.1. Traverse 1

The 2-D electrical resistivity subsurface structure along traverse 1 is characterised by three different resistivity responses; low resistivity response (generally < 120 Ohm-m), intermediate resistivity responses (resistivity in the range 130– 575 Ohm-m) and high resistivity responses having resistivity above 1000 Ohm-m. It displayed the low resistivity response at the surface at locations 53– 103 m, 160– 303 m and 350– 425 m. This extends beyond 20 m depth at location 53– 103 m (Figure 18a). This low response is located within a trough at the top of intermediate resistivity responses below at 160– 303 m and 350–425 m. A deep weathering zone at 53– 103 m with low resistivity (Figure 18a) indicating fracture could pose threat to civil engineering works at the site. The intermediate resistivity response of 130– 575 Ohm-m extends throughout the traverses occurring between the low resistivity and high resistivity responses with the exception of 53– 103 m. It's shown at the surface before 20– 53 m, 103– 163 m, 303– 350 m and 425 m till the traverse end. At locations 120– 135 m and 300– 330, the response extends to the depth above 20 m. The high resistivity response cut across the section continuously extending from 25– 360 m except where it is segmented by a low resistivity deep weathering/fracture section between 53– 135 m and 300– 330 m. Between 160– 303 m, its upper surface forms a large trough filled with low resistive materials. The high resistivity responses dominate the northwestern part to the central part of the section, until it

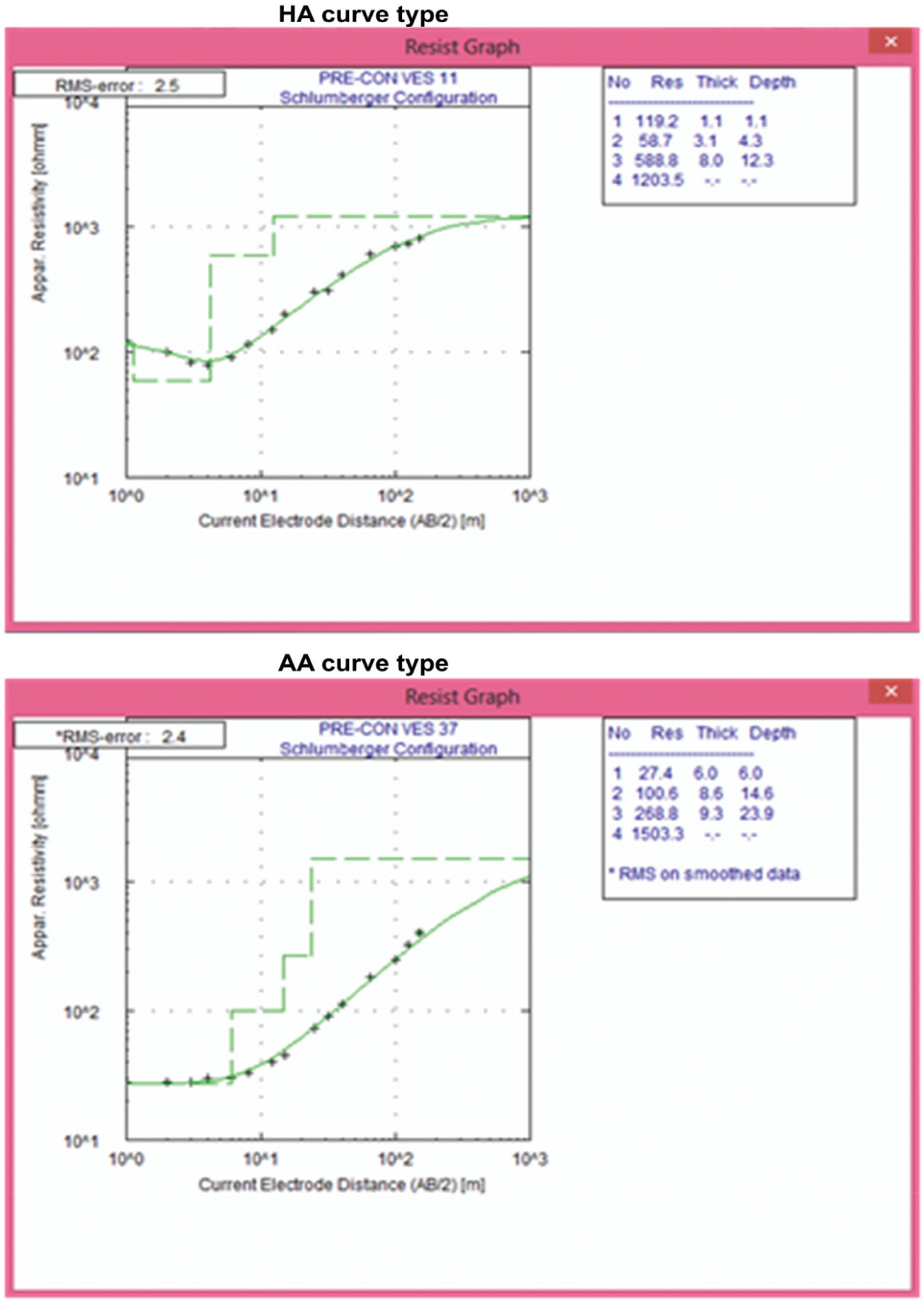

Figure 17. Representative curve types of the site.

terminates at approximately 75– 135 m with a vertical edge indicative of the presence of fracture. The low resistive portions on the 2-D subsurface structure are coincident with the weathered layer on the geoelectric section. Also, the subsurface features on the inverted 2-D resistivity structure are coincident with the features on VLF-EM 2-D section. Four distinctive geologic layers are delineated (Figure 18b). The top layer is characterised by resistive formation (238– 350 Ohm-m) of sand/lateritic sand, 1.1– 1.4 m thick. The composition of the thick (4.6– 7.4 m) weathered/regolith unit is entirely clay (47– 56 Ohm-m). The clay composition of the weathered layer with < 60 Ohm-m indicates water saturation of the zone. This clay composition and water saturation of the subsoil are potential threat to the proposed civil engineering works. The low resistivity clay weathering materials along the traverse coincide with the high conductivity zones in the bedrock. The basement topography is irregular and forms depression at VES station 2 with depth to bedrock from 13.6 (VES 5) – 18.5 m (VES 2) (Figure 18b). Bedrock depression is a typical groundwater collecting zone in form of trough, receiving water discharging from the crest. The basement depression is overlain by highly conductive layers (clay), thus unsuitable to sustain substantial civil engineering structures. The partially weathered/fractured basement (261– 467 Ohm-m) with thickness range

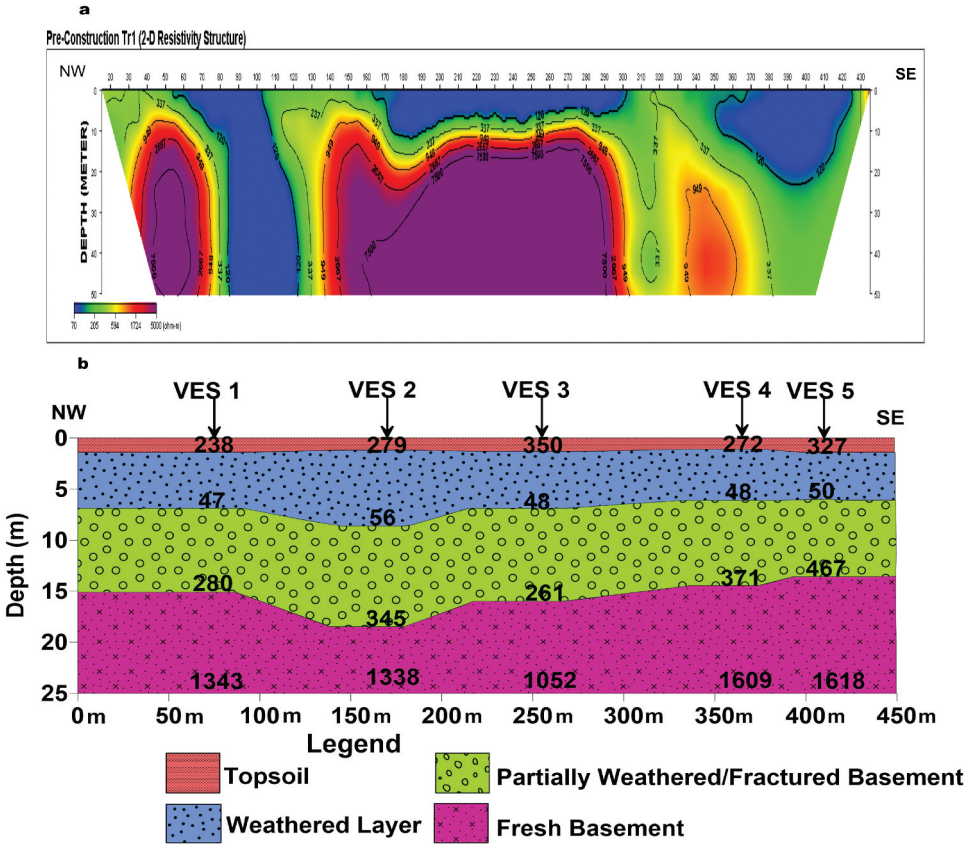

Figure 18. (a) Two-dimensional (2D) subsurface structure (b) geoelectrical section obtained from VES curves 1 to 5 of Traverse 1.

7.6– 9.9 m cut across all the VES stations of this location. Resistivity values of this layer beneath the weathered layer indicate water-saturated fractured bedrock. Its existence with the basement depression constitutes potential weak zones that could pose a threat to the stability of the engineering projects. The fresh bedrock possesses resistivity 1052– 1618 Ohm-m (Figure 18b). Classified incompetent zones may expose the various proposed civil works to future failure, if necessary precautionary measures are not taken to mitigate future challenges. From the geologic setting of this location, soils at shallow depth are unsuitable as foundation geo-materials. Thus, shallow foundation type is not encouraged as the overburden thickness increases significantly with water saturated subsoil, which could result to subsidence/differential settling that poses risk to foundation of buildings resulting to failure even shortly after construction. Deep foundations in form of piers and piles are encouraged to transmit structural load to competent and reliable fresh bedrock for safe and stable construction except in cases of soil stabilisation.

4.2.2. Traverse 2

Subsurface image along traverse 2 is also characterised by the three different resistivity responses (Figure 19a). Low resistive response occurred at the surface 30– 205 m, 230– 240 m, 250– 315 m and 410– 512 m with resistivity values below 120 Ohm-m, indicative of deep weathering sections characterised by clayey subsoil within the bedrock. This response extends beyond 20 m depth at location 250– 315 m (Figure 19a). The low resistivity response is located within a trough at the top of intermediate resistivity responses below at 40– 205 m and 430– 512 m. The subsurface near vertical low resistivity weathered features at the location 250– 315 m indicate fracture, saturated clay, bedrock depression or geologic contacts (Figure 19a). This low resistivity deep weathering at 250– 315 m could be problematic as it conduits groundwater through the site. Potential failure of the buildings may be influenced by this near surface incompetent clayey materials and near-vertical geological features like fracture, lithological contact and basement depressions (Figure 19a). The intermediate resistivity response (130– 575 Ohm-m) extends throughout the traverse occurring between the low resistivity and high resistivity responses with the exception of 250– 315 m. This resistivity response dominates the section and shown at the surface before 20– 40 m, 205– 250 m, 315– 405 m and 512 m towards the traverse end (600 m). The response extends beyond the depth of 20 m on the section where it occurs except at 205– 250 m. The high resistivity response extends beyond the depth

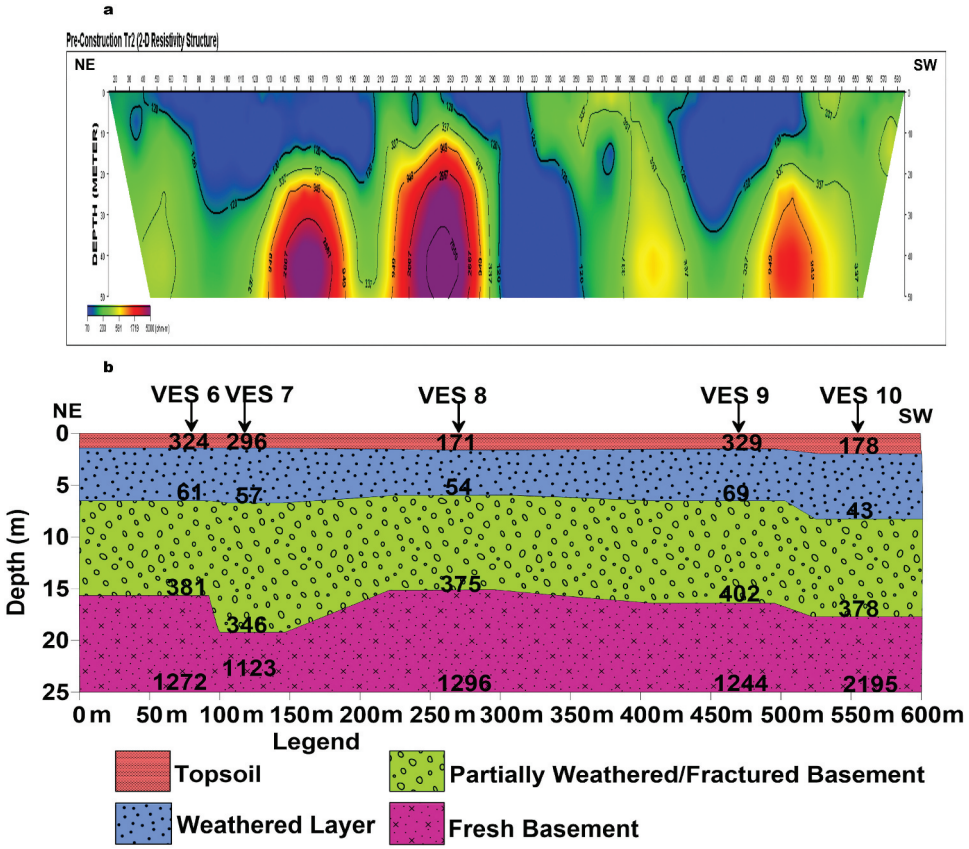

Figure 19. (a) Two-dimensional (2D) subsurface structure (b) geoelectrical section obtained from VES curves 6 to 10 of Traverse 2.

of 20 m below the surface forming dome-like basal high resistivity response at 130– 185 m, 215– 280 m and 490– 520. Between 40– 205 m and 410– 512 m, its upper surface forms a large trough filled with low resistive materials. The low resistive portions on the 2-D subsurface structure coincide with the weathered layer on the geoelectric section, indicative of saturated clayey zones. Also, the subsurface features on the inverted 2-D resistivity structure are coincident with the features on VLF-EM 2-D section. Four lithologic layers are distinguished at this location (Figure 19b). The resistive topsoil (171– 329 Ohm-m) with thickness in the range 1.4– 2.0 m corresponds to sand/lateritic sand. The composition of the weathered basement is clay, having resistivity in the range 43– 69 Ohm-m and 4.5– 6.2 m thickness. Resistivity range of < 70 Ohm-m of this unit is an indication of water saturation of the clay materials. Saturated clayey nature of the subsoil poses potential threat to the proposed building foundation. The water saturated clay along this traverse coincident with the high conductivity zones trending in different directions across the section. The topography is irregular which forms depression at VES station 7 with depth to bedrock from 15.1 (VES 8) – 19.2 m (VES 7) (Figure 19b). The basement depression is overlain by highly conductive layers of saturated clay, thus unsuitable to sustain the proposed civil engineering structures. The partially weathered/fractured basement has resistivity and thickness range 346– 402 Ohm-m and 9.1– 12.6 m respectively, which cut across all the VES stations at this location. Resistivity values of this layer indicative water-bearing fractured basement which form a viable site for groundwater development with maximum yield. This layer therefore forms an incompetent layer for building construction which could result to subsurface subsidence and differential settling of the subsoil with resultant building failure. The existence of this layer and the basement depression constitute potential weak zones that would threaten stability of civil engineering structures constructed on it. The fresh bedrock is with resistivity 1123– 2195 Ωm (Figure 19b). Those categorised incompetent layers would expose the proposed earthworks to failure, if necessary precautionary measures are not put in place to mitigate future challenges. Soils at shallow depth at this location are unsuitable layer for foundation. Hence, shallow foundation is not encouraged because there is likelihood of subsurface subsidence and differential settlement for structures constructed on the soils. Deep foundations in form of

piers and piles are encouraged for safe and sustainable construction except in cases of soil stabilisation.

4.2.3. Traverse 3

The 2-D resistivity image of the subsurface along traverse 3 displayed three resistivity responses (Figure 20a). The low resistivity response occurred at the surface before 20– 32 m, 97– 252 m, 306– 366 m and 403– 530 m with resistivity values below 120 Ohm-m, indicative of deep weathering sections characterised by clayey subsoil within the bedrock. This response extends beyond 20 m depth at location 120– 160 m, 200– 260 m and 358– 385 m (Figure 20a). The low resistivity response is located within a trough at the top of intermediate resistivity responses across the section. The near-surface vertical low resistivity weathered features at the location 306– 366 m indicate the presence of a fracture (Figure 20a) which could pose threat to civil engineering works at the site. Failure of the buildings would be influenced by the near surface incompetent clayey subsoil and near-vertical geological features like fracture, lithologic contact and basement depressions (Figure 20a). The intermediate resistivity response 130– 575 Ohm-m extends throughout the traverse. This response reflects across the section below the trough filled with low resistive materials but intrudes to the surface at some points of the location. The high resistivity response extends beyond the depth of 20 m below the surface forming dome-like high resistivity bodies beneath the intermediate resistivity zones at approximately 85– 200 m, 280– 350 m and 400– 540 (Figure 20a). The low resistive portions on the 2-D subsurface structure coincide with the weathered layer on the geoelectric section, indicative of saturated clayey zones. Also, the subsurface features on the inverted 2-D resistivity structure are coincident with the features on VLF-EM 2-D section. Four lithological units are established at this location. The resistivity of the topsoil varies from 97– 357 Ohm-m and thickness, 0.7– 1.7 m corresponds to clay/sandy clay/clayey sand/lateritic sand. The weathered basement composed majorly of clay (59– 129 Ohm-m) and thickness range 3.1– 14.6 m (Figure 20b). The resistivity range of < 75 Ohm-m except beneath VES 14 of this unit is an indication of water saturated clay materials. Saturated clayey nature of the subsoil poses potential threat to building foundation. The water saturated clay along this traverse coincident with the high conductivity zones trending in different directions across the section. The topsoil and weathered layer (subsoil) are largely composed of clay (resistivity values < 130 Ohm-m) with clayey sand/lateritic sand in place as topsoil beneath VES stations 12 and 13 with resistivity values > 200 Ohm-m (Figure 20b). The clay composition of the weathered layer indicates water saturation of the zone. Clayey and water saturated subsoil are incompetent layer that cannot support the proposed civil works. The basement topography is irregular and forms depression at VES station 12 with depth to bedrock

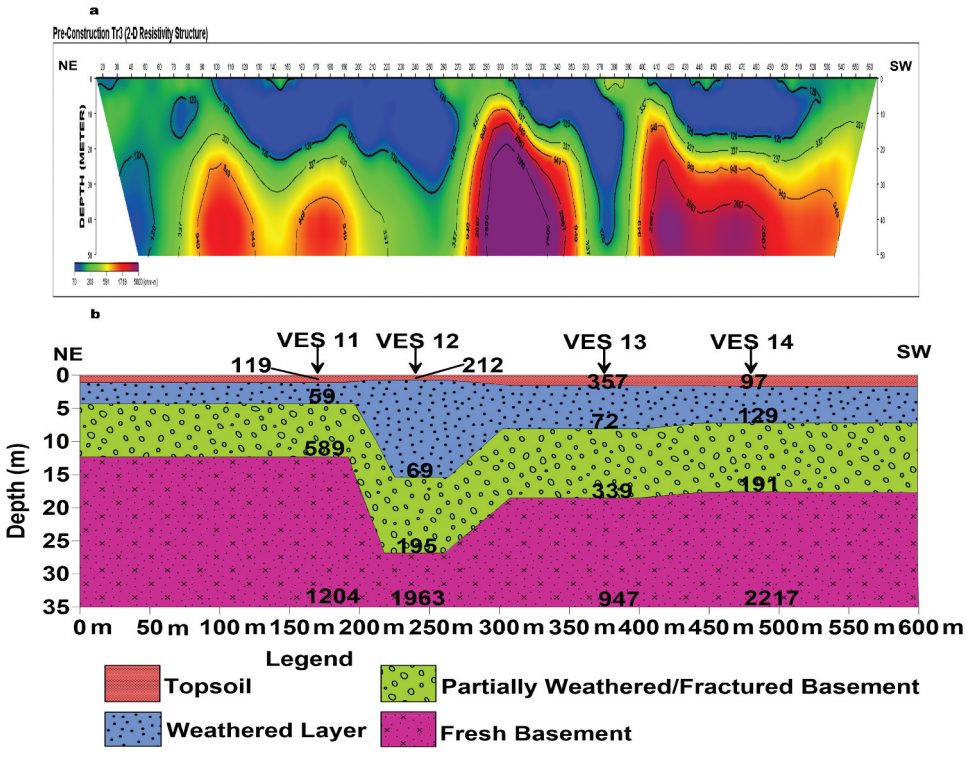

Figure 20. (a) Two-dimensional (2D) subsurface structure (b) geoelectrical section obtained from VES curves 11 to 14 of Traverse 3.

from 12.3– 26.8 m (Figure 20b). The partially weathered/fractured basement (191– 589 Ohm-m) and range of thickness 8.0– 11.5 m, cut across all the VES stations at this location. Resistivity values of this layer indicate water-bearing fractured basement which form groundwater potential zone within the location. Thus, the weathered basement and fractured/ partially weathered bedrock form two main aquiferous units in the area. Taking into consideration the resistivity value of aquifer units and its overburden thickness, VES 12 signifies a viable groundwater potential zone in the area for sustainable groundwater development. These layers therefore are incompetent for building construction because they could result to settling of parts of the building constructed on it. Also, interaction of the subsoil which form foundation base with water would reduce its load bearing capacity. The existence of these layers and the basement depression constitute potential weak zones that would threaten stability of civil engineering structures at the site. The fresh bedrock has resistivity values varying from 947– 2217 Ohm-m (Figure 20b). The classified incompetent layers would contribute to the failure of proposed earthworks if not properly considered during the foundation design and construction to mitigate future challenges. The identified incompetent layers may pose risk to building. From the study of this location, future failure of earthworks may arise from the existence of concealed geologic structures and inhomogeneous subsurface settings as a result of abrupt changes in resistivity values.

4.2.4. Traverse 4

The 2-D resistivity image of the subsurface along traverse 4 displayed three resistivity responses (Figure 21a). The low resistivity response with resistivity values below 120 Ohm-m is identified at the surface between 40– 60 m, 100– 202 m and 248– 364 m, indicative of clayey subsoil within the bedrock. This response at location 140– 170 m and 310– 350 m extends beyond 20 m depth (Figure 21a). The low resistivity response is located within a trough at the top of intermediate resistivity responses across the section at 100– 202, which coincide with the identified fracture, F7–F7′ on the VLF-EM 2-D section. The near-surface vertical low resistivity weathered features at the location approximately 250– 364 m indicate the presence of a fracture (Figure 21a). The intermediate resistivity response dominates the section. It cuts across

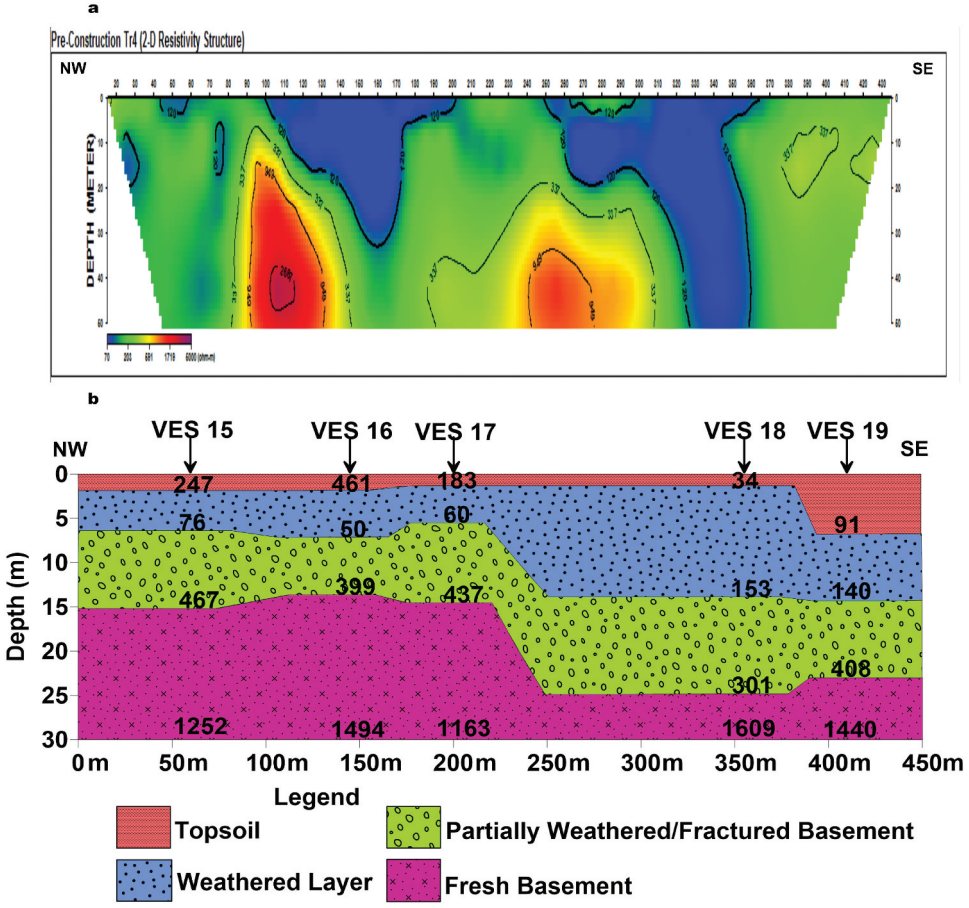

Figure 21. (a) Two-dimensional (2D) subsurface structure (b) geoelectrical section obtained from interpretation of VES curves 15 to 19 along Traverse 4.

the section of the traverse and between the low resistivity and high resistivity responses at 250–364 m, where it is observed below the trough filled with low resistive materials but intrudes to the surface at some other points of the location. The high resistivity response extends beyond 20 m depth forming dome-like basal high resistivity bodies beneath the intermediate resistivity zones at approximately 90– 135 m and 240– 290 (Figure 21a). The low resistive portions on the 2-D subsurface structure coincide with weathered bedrock, indicative of saturated clayey zones. The intermediate resistivity responses are coincident with the partially weathered/fractured basement on the geoelectric section. Also, the subsurface features on the inverted 2-D resistivity structure are coincident with the features on VLF-EM 2-D section. Traverse 4 shows four geologic units (Figure 21b), resistivity of the topmost layer varies from 34– 461 Ohm-m with thickness range 1.3–6.8 m corresponds to clay, clayey sand and lateritic sand. The weathered bedrock is majorly clay (50–153 Ωm) and thickness range of 4.2– 12.6 m (Figure 21b). The resistivity range of < 80 Ohm-m except beneath VES stations 18 and 19 is an indication of water saturated clayey subsoil. The water saturated clay along this traverse coincident with the high conductivity zones trending in different directions across the section. The topsoil and weathered layer (subsoil) are largely composed of clay and clay composition of the weathered layer indicates water saturation of the zone. Saturated clayey nature of the subsoil is an incompetent layer that cannot support the proposed civil works, thus, poses potential threat to building foundation due to exposure to excessive water leading to strength reduction of the soils. The basement relief is irregular and forms depression at VES station 18 with depth to bedrock from 13.6–24.8 m (Figure 21b). The resistivity values of the third unit in the range 301– 467 Ohm-m with thickness range of 6.8– 11.0 m lies beneath the weathered layer in all the VES stations of the location. Resistivity values of this layer indicate water-bearing fractured basement which form groundwater potential zone within the location. Thus, the weathered basement and partially weathered /fractured basement form the two main aquiferous units in the area. Relative to the resistivity value of aquifer units and its overburden thickness, VES 18 serves as a suitable groundwater potential zone in the area for sustainable groundwater development. These layers form incompetent zones for building construction which may result to subsurface subsidence and differential settlement. Building constructed on these classified aquiferous unit would definitely collapse as the interaction of the subsoil with water would result to reduction of the load bearing capacity of the soil, thus stability of the civil engineering structures constructed on it is not guaranteed. Failure of the buildings would be influenced by the near surface incompetent clayey subsoil with existence of subsurface structures; fracture, basement depressions and lithologic contact (Figure 21b). The classified incompetent layers would contribute to the failure of proposed earthworks if not properly addressed during the foundation design and construction, to prevent future failure. From this study, future failure of engineering structures may arise from the existence of concealed geologic structures like faults, fractures and inhomogeneous subsurface units as a result of abrupt variations in resistivity values of the location.

4.2.5. Traverses 5 and 6

Four different lithologic units are determined on traverses 5 and 6 (Figure 22). The resistivity of the uppermost layer varies from 77 to 307 Ohm-m with thickness in the range 0.8–9.5 m corresponds to clay, sandy clay and clayey sand/lateritic sand. The weathered layer is majorly clay with resistivity range of 51–175 Ohm-m and thickness range of 3.4–12.3 m (Figure 22). This clayey geomaterial in the weathered layer suggests low resistivity water saturated zone. The topsoil and water saturated unit (weathered layer) are largely clayey with resistivity values <176 Ohm-m except beneath VES station 24 only with resistivity value of 307 Ohm-m, indicative of water absorbing clayey subsoil. The soils at shallow depth of these locations are poor geo-engineering materials for foundation. The low resistivity clay weathering materials along the traverses coincide with the high conductivity zones in the bedrock. Bedrock depression is groundwater storage zone in the form of trough, receiving water flowing down freely from the crest and it is overlain by high conductive units/low resistive materials (clay). The basement relief is irregular and forms depression at VES station 21 with the thickest overburden at the location. The depth to bedrock varies from 11.8 (VES 24) to 31.7 m (VES 22) (Figure 22). The low resistive saturated layer and basement depression in the locations are subsurface structures favourable for groundwater development, but they are incompetent zones unsuitable to sustain and support substantial civil engineering earthworks, as they pose threat to structural stability. The partially weathered/fractured basement with resistivity varying from 360 to 510 Ohm-m and thickness range of 7.6 to 10.0 m cut across all the VES stations of the locations. The established incompetent regions identified as conductive zones, linear conductive

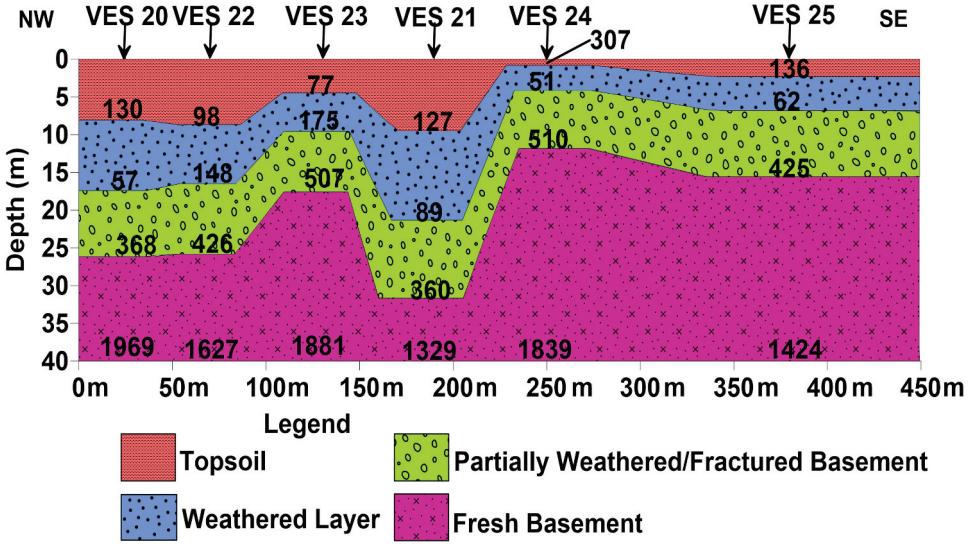

Figure 22. Geoelectrical section of Traverses 5 and 6.

features; fractures (F8–F8′ and F9–F9′) from the VLF-EM 2-D inverted models, basement depression and the low resistive saturated units from the geoelectric section are inimical to structural earthworks. Possible failure of the proposed building may arise from concealed subsurface structures and abrupt lateral inhomogeneous geologic units as a result of large resistivity variations. The classified incompetent zones may expose the proposed construction works to future failure if necessary preventive measures are not put in place especially during structural design and construction to mitigate the future challenges. Soils at shallow depth <12.5 m are not suitable for building foundation; thus, shallow foundation is not encouraged because there is a possibility of differential settlement to structures constructed on soils at such depth. Deep foundations, except in cases of soil stabilisation in the form of piers and piles, are encouraged.

4.2.6. Traverses 7, 8 and 9

Four lithologic units are present in this area (Figures 23 and 24). The resistivities of the top layer vary from 183–507 Ohm-m along traverse 7 (Figure 23), 34–326 Ohm-m along traverses 8 and 9 (Figure 24) with thicknesses, 0.8–1.6 m and 0.6–4.7 m, respectively. The resistivities signify clay/sandy clay/clayey sand/lateritic sand. The weathered layer composed majorly of clay with resistivity range of 54–70 Ohm-m along traverse 7, 62–143 Ohm-m along traverses 8 and 9 with thicknesses in the range of 2.6–6.4 m and 2.6–7.2 m, respectively (Figures 23 and 24). The resistivity range of <105 Ohm-m of this unit with the exception of VES 34 is an indication of water saturation in the clay materials. The resistivity value of VES 34 in the weathered layer is 143 Ohm-m, characterised by sandy clay. Clayey and water saturated subsoil are incompetent layer that cannot support

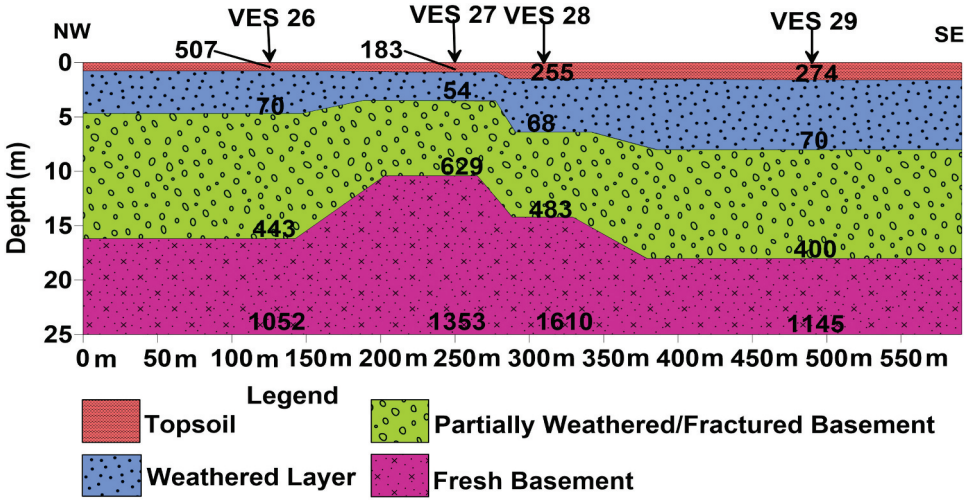

Figure 23. Geoelectrical section of Traverse 7.

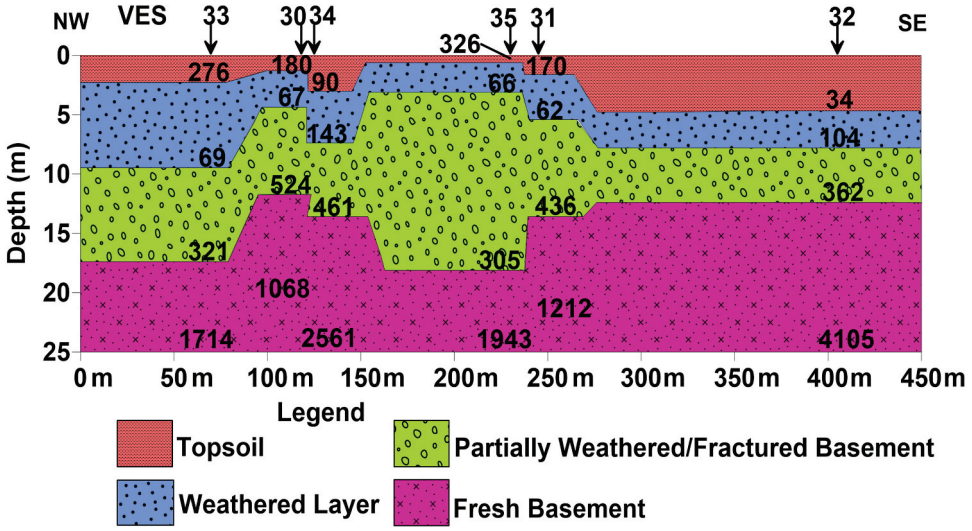

Figure 24. Geoelectrical section of Traverses 8 and 9.

civil works. Saturated clayey nature of the subsoil could negatively impact the integrity and stability of the building foundation. The water saturated clay along these traverses coincident with the high conductivity zones trending in different directions across the sections. The bedrock topography is irregular and forms depressions at VES stations 26, 29, 33 and 35 with depth to bedrock from 10.4 to 18.0 m and 11.7 to 18.1 (Figures 23 and 24). Bedrock depressions identified at some points of the study area could also threaten the foundation stability of the construction works causing differential settlement of the earthworks. The depressions are good groundwater potential zones but inimical to engineering earthworks. Thus, to avert the threat of ground variations, foundation should be designed to rest on competent rock layer. The third layer of the locations has resistivity variations of 400–629 Ohm-m and 305–524 Ohm-m and thickness range of 6.4–11.4 m and 4.6–14.9 m, which cut across all the VES stations at the locations. The weathered and partially weathered/fractured bedrock form two main aquiferous units of the area. Thus, taking into consideration the resistivity values of aquifer units and its overburden thickness, VES 26, 29, 33 and 35 are viable groundwater potential zones for maximum productivity and sustainability to enhance groundwater development in the area. These layers are incompetent subsoil layers that would permit interaction of foundation soil with water with reduction of load bearing capacity of the soil, posing risk of subsidence to construction earthworks within the survey area. The fresh bedrock is characterised by resistivity 1052–1610 Ohm-m (traverse 7) and 1068–4105 Ohm-m (traverses 8 and 9) (Figures 23 and 24). The classified incompetent layers would contribute to the failure of proposed earthworks if not properly considered during the foundation design and construction to mitigate future challenges. Resistivity values of subsoil strata dictate its engineering suitability; thus, the fresh basement is considered as sound and competent layer for the building constructions within the area. Future failure of engineering structures may arise from the existence of concealed geologic structures like faults, fractures, bedrock depressions and heterogeneous subsurface units. Thus, soils at shallow depth at these locations are unsuitable for foundation. Shallow foundation is not encouraged because there is likelihood of differential settlement and to avert the risk of structural failure after construction, deep foundations except in cases of soil stabilisation in the form of piers and piles are encouraged for sustainable construction.

4.2.7. *Traverses 10, 11, 12 and 13*

Four major lithologic units are distinguished in this area (Figures 25 and 26). The resistivities of the topsoil vary from 27–466 Ohm-m along traverses 10 and 11 (Figure 25), 219–456 Ohm-m along traverses 12 and 13 (Figure 26) with thicknesses, 1.4–6.0 m and 1.2–2.5 m, respectively. The resistivities indicate clay, sandy clay and clayey sand and lateritic sand. The weathered basement corresponds to clay with resistivity range of 30–130 Ohm-m along traverses 10 and 11 and 21–73 Ohm-m along traverses 12 and 13 with thicknesses in the range of 4.0–9.5 m and 4.0–9.8 m, respectively (Figures 25 and 26). The resistivity range of subsoil ≤130 Ohm-m of this unit is indicative of water saturation in the clay materials. Clayey and water saturated subsoil are incompetent layer that cannot support civil works. Saturated clayey nature of the subsoil could negatively impact the

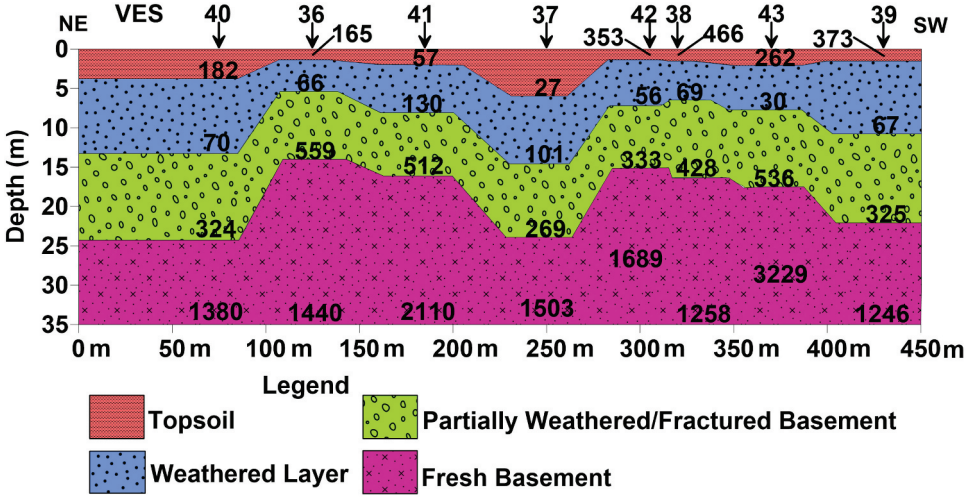

Figure 25. Geoelectrical section of Traverses 10 and 11.

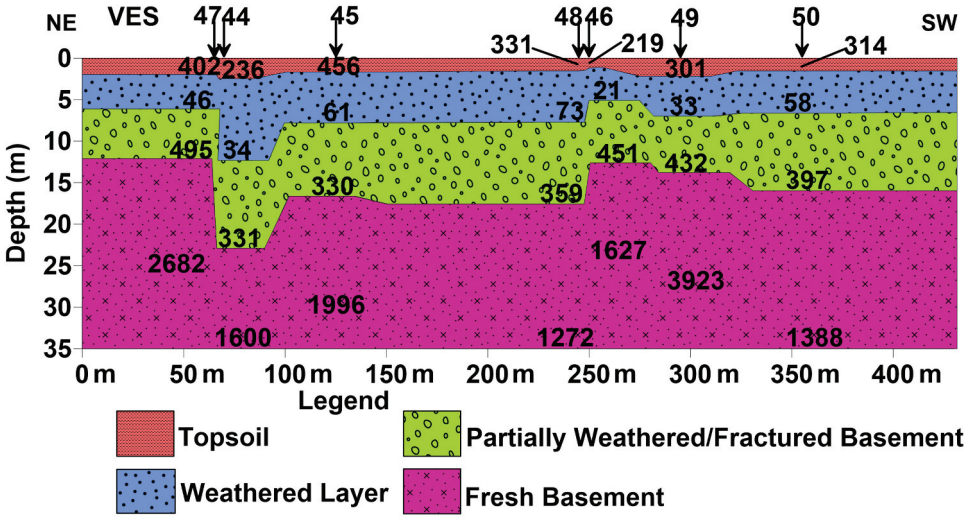

Figure 26. Geoelectrical section of Traverses 12 and 13.

integrity and stability of the building foundation. The water saturated clay along these traverses coincident with the high conductivity zones trending in different directions across the sections. The basement topography is irregular and forms depressions at VES stations 37, 39, 40, 44, 48 and 50 with depth to bedrock from 14.0 to 24.3 m and 12.1 to 22.9 m (Figures 25 and 26). Bedrock depressions identified at some points could threaten earthworks foundation stability causing its differential settlement. These depressions are good groundwater potential zones but inimical to engineering construction works. Thus, the threat of ground variations can be prevented, if structural foundations are designed to rest on competent rock layer. The partially weathered/fractured basement of the locations has resistivity variations of 269–559 Ohm-m (Figure 25) and 330–495 Ohm-m and thickness range of 8.0–11.4 m and 6.2–10.6 m, which transpire across all the VES stations of the locations. Resistivity values of this layer indicate water saturated fractured basement which constitute groundwater potential zone within the locations. Thus, taking into consideration the resistivity values of aquiferous units (weathered and fractured/partially weathered bedrock) and its overburden thickness, VES 37, 39, 40, 44, 48 and 50 are viable groundwater potential zones for maximum yield and sustainable groundwater development in the area. These layers are incompetent subsoil layers that would permit interaction of foundation subsoil with water with potential to pose threats to construction earthworks within the survey area. The fresh bedrock has resistivity values varying from 1246 to 3229 Ohm-m (traverses 10 and 11) and 1272 to 3923 Ohm-m (traverses 12 and 13) (Figures 25 and 26). The categorised incompetent layers would contribute to failure of the proposed civil-works if necessary preventive measures are

not put in place during foundation design and construction to mitigate future challenges. Resistivity values of subsoil strata dictate its engineering suitability; thus, the fresh basement is considered as sound and competent layer for the building constructions within the area. Future failure of engineering structures may arise from the existence of concealed geologic structures like faults, fractures, bedrock depressions and heterogeneous subsurface layers. Soils at shallow depth at these locations are unsuitable for foundation building. Shallow foundation is not encouraged for buildings within the area because there is likelihood of differential settling which can also pose considerable threat to the engineering structures after construction. Thus, for sustainable structural development in order to prevent the risk of structural failure in the area, deep foundation works in the form of piers and piles are recommended except in cases of soil stabilisation.

The direction of groundwater flow identified aid to establish the discharge zones or groundwater high-yield zones which are detrimental to foundation works (Ademila and Saloko 2018). The surface elevation map (Figure 27a) demonstrates that groundwater moves from north to the south and northeastern regions to southwestern parts of the study area. The 3-D elevation map (Figure 27b) shows the topographic characteristics of the study area with the depressions serving as the groundwater storage centres within the area. The topographical high zones are the recharge points, while the topographical lows are the discharge areas. This suggests that structural foundations should be erected towards the northern and northeastern flank to prevent water ingress into foundation works and avert future structural failure.

4.3. Subsurface characterisation

Resistivity values of subsurface units dictate its engineering suitability and soil corrosivity classified based on resistivity of soil (Agunloye 1984; Baeckmann and Schwenk 1997), showed that low soil resistivity has impact on corrosivity of buried metallic pipes (part of building materials). The soil layer accommodating buried pipes must be non-corrosive otherwise the buried metallic pipes would rust, thus, failure of engineering structures in the area. High conductivity/low resistivity geologic unit is a good electrical conductor resulting to reduction in aeration. The depth of buried pipes usually do not exceeds 3 m, which is within subsoil layers of the study area with resistivity in the range 21– 507 Ohm-m (Figures 28 and 29) and thickness variation of 0.6– 14.6 m, indicating corrosive to practically non-corrosive. The buried metallic engineering construction works at some locations within the site would be at risk of being

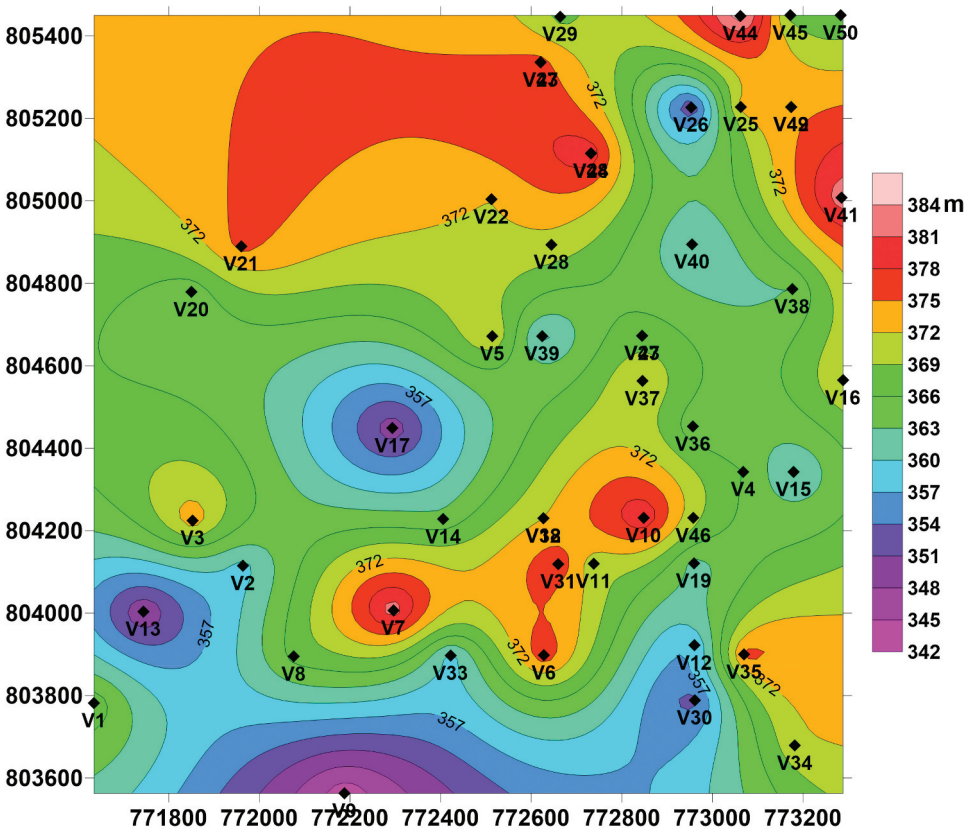

Figure 27. (a) Surface elevation view of the area. (b) 3D elevation view of the area.

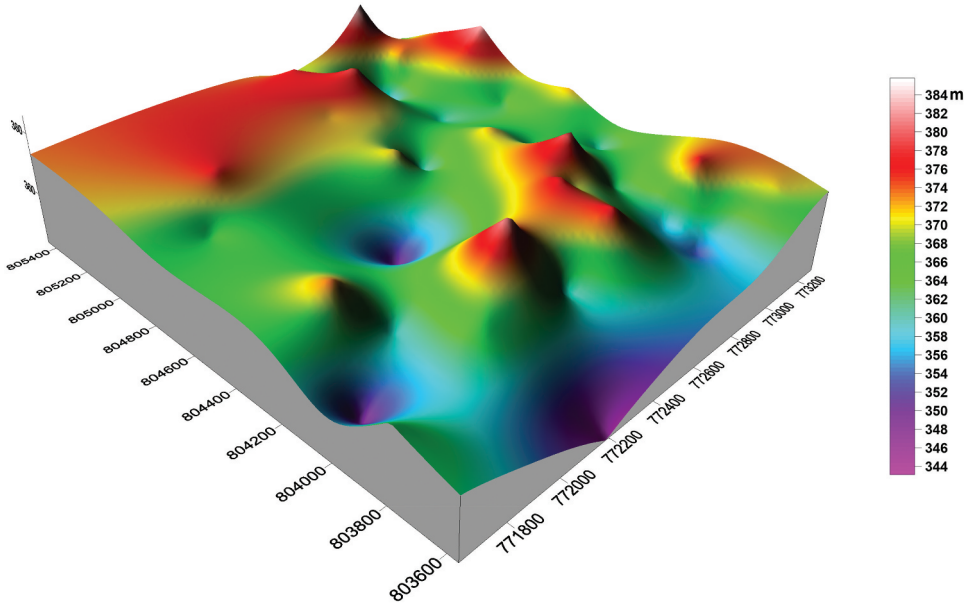

Figure 27. Continued.

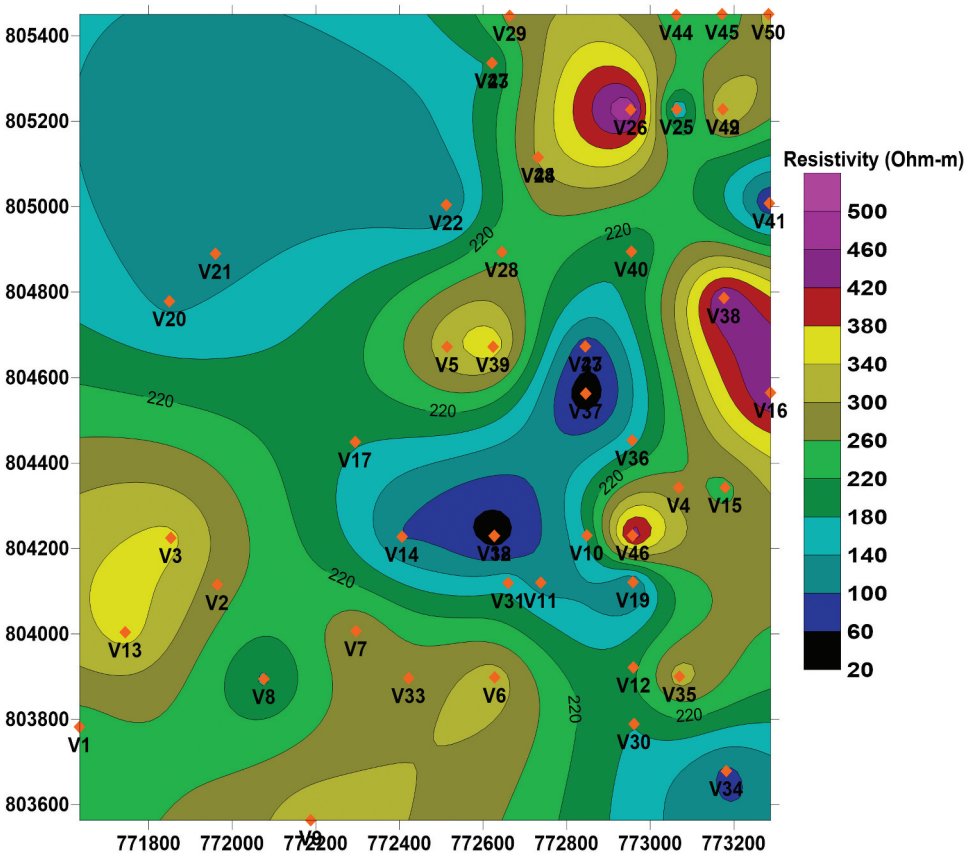

Figure 28. Resistivity distribution of topsoil of the site.

corroded. Thus, the fresh bedrock with higher resistivity is considered as sound and competent layer for the building constructions within the area shown on the fresh bedrock resistivity map of the site (Figure 30a). Foundation of various civil-works in the site should be designed to rest on competent bedrock (Figure 30a) for sustainable infrastructural development. 3-D map of the fresh bedrock resistivity of the site (Figure 30b) shows the variations of high layer resistivity which are good site for safe and sustainable construction, while that of low resistivity values are good

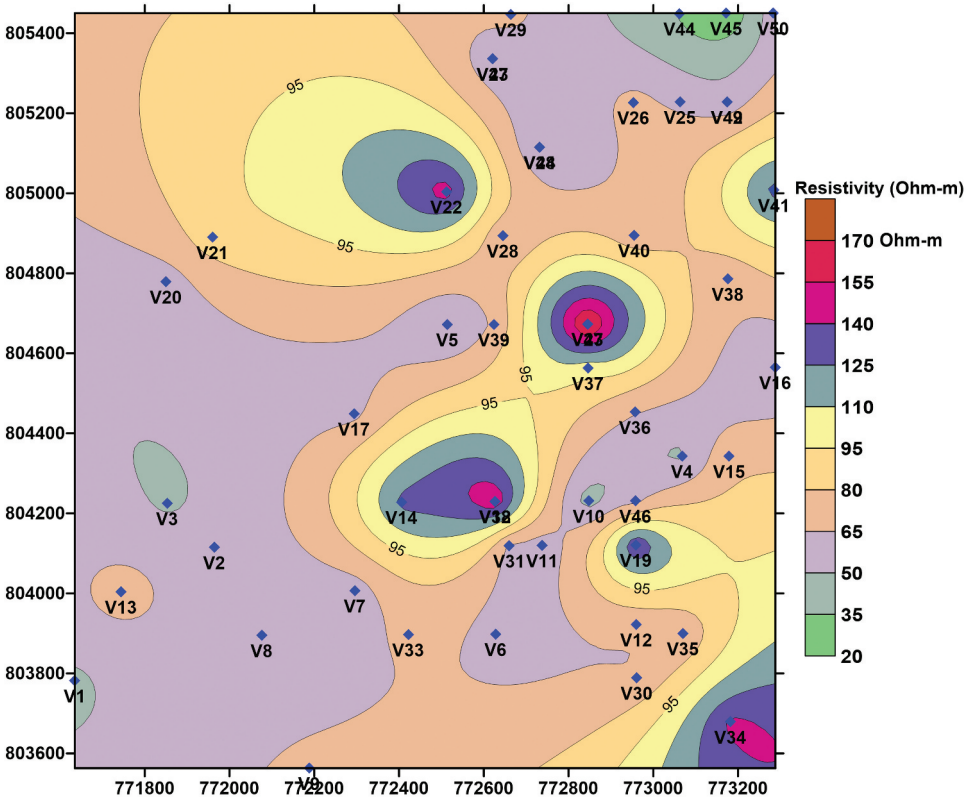

Figure 29. 2-D resistivity view of weathered basement of the engineering site.

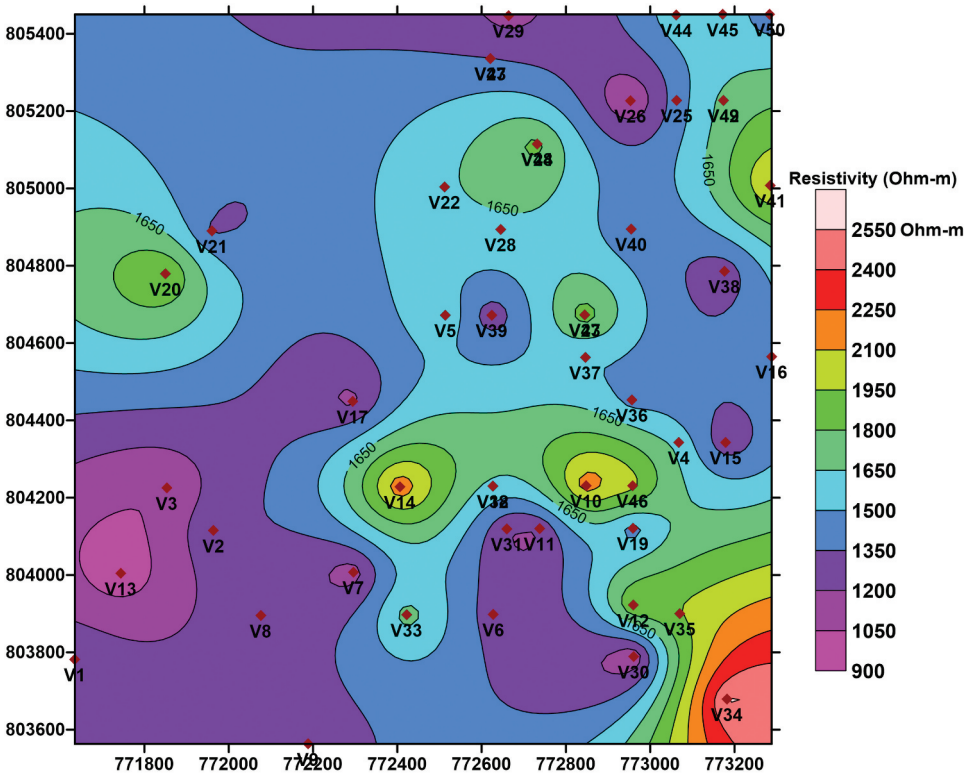

Figure 30. (a) Fresh bedrock resistivity map of the engineering site. (b) 3D perspective resistivity view of the fresh bedrock of the site.

groundwater potential zones, disastrous to foundation of engineering structures. Deep foundation works are encouraged in form of piers and piles except in cases of soil stabilisation for stable engineering structures. Documentation of the results of this study is recommended for foundation

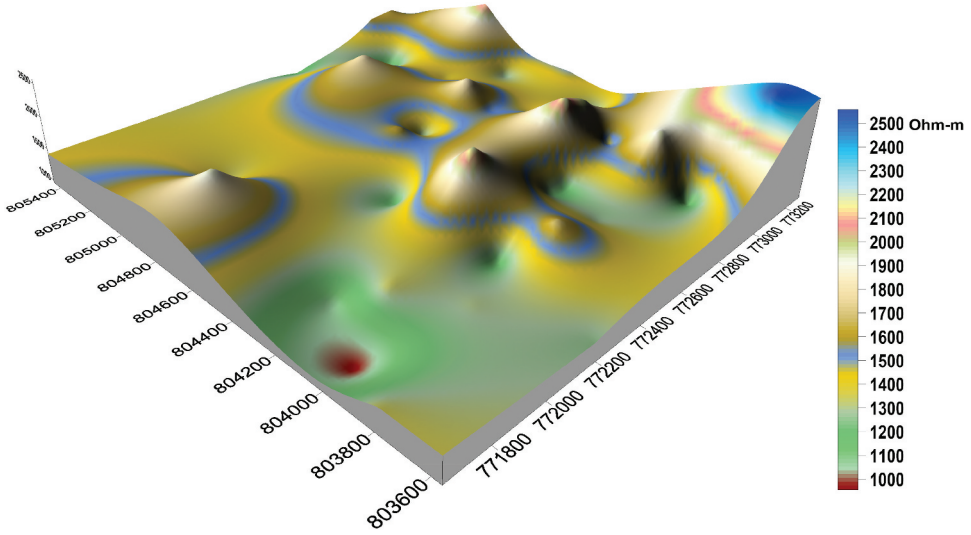

Figure 30. Continued.

design and construction on the site and future development of other engineering sites. Structural characterisation map is usually useful in engineering, environmental geophysics and groundwater studies, fracture zones in this area are distributed over the observed geologic units, cross cutting in different directions and show their lithologic boundaries (Figure 31). These features resulting from deformation of underlying parent rock are indicators of subsurface geological structures incompetent for civil engineering construction works due to its negative impact on foundation stability. Considering the results from the VLF-EM and electrical resistivity given in this study, it can be concluded that the two techniques are efficient in subsurface characterisation of a site for sustainable engineering construction works, revealing information on nature of the subsurface geological setting. The major problem discovered in this geophysical study is the existence of geological structures, uneven bedrock topography with depressions filled with low resistive geo-materials, deep weathering and fracturing of bedrock and saturated clayey subsoil in some locations. The engineering site with undulating bedrock topography is classified into stable and unstable sections (Figure 32) following the results of the study. The stable section is considered as sound and competent layer for the building constructions within the area and recommended for substantial engineering structures coupled with the use of standard quality construction materials. The unstable sections constitute the deep weathering sections of the survey area with potentially unstable geologic materials that tend to conduit groundwater through the engineering site. They are considered as unsuitable/incompetent zones that cannot sustain civil works and should be avoided by the building developers/building contractors to avert the risk of structural failure. The presence of concealed geologic structures beneath the unstable section could lead to differential settling which poses threat to civil-works at the site. The established unstable section would contribute to failure of the proposed civil-works if necessary preventive measures are not put in place during foundation design and construction to mitigate future challenges. It is recommended that foundation of buildings should not be constructed on classified unstable zones. This bedrock topography should be taken into consideration and used as basis for design or construction planning of engineering structures in the site and to provide preventive measures against the risk of building failure.

5. Conclusion

VLF-EM electromagnetic and electrical resistivity techniques involving vertical electrical resistivity sounding and 2-D electrical resistivity imaging have been successfully utilised in the characterisation of subsurface geological setting of a site for sustainable structural development. This study was to give detailed information on the existence of subsurface geological structures with possible engineering threat to proposed buildings. This is viewed to help in decision-making on the suitability of the area for construction and design effective structural foundations for sustainable building constructions. The VLF-EM mapped conductive zones, fractures (F–F', F1–F1′ to F16–F16′ and F16") which are unfavourable to engineering construction works. These characteristic weak zones constitute structural instability in complex geological terrain if

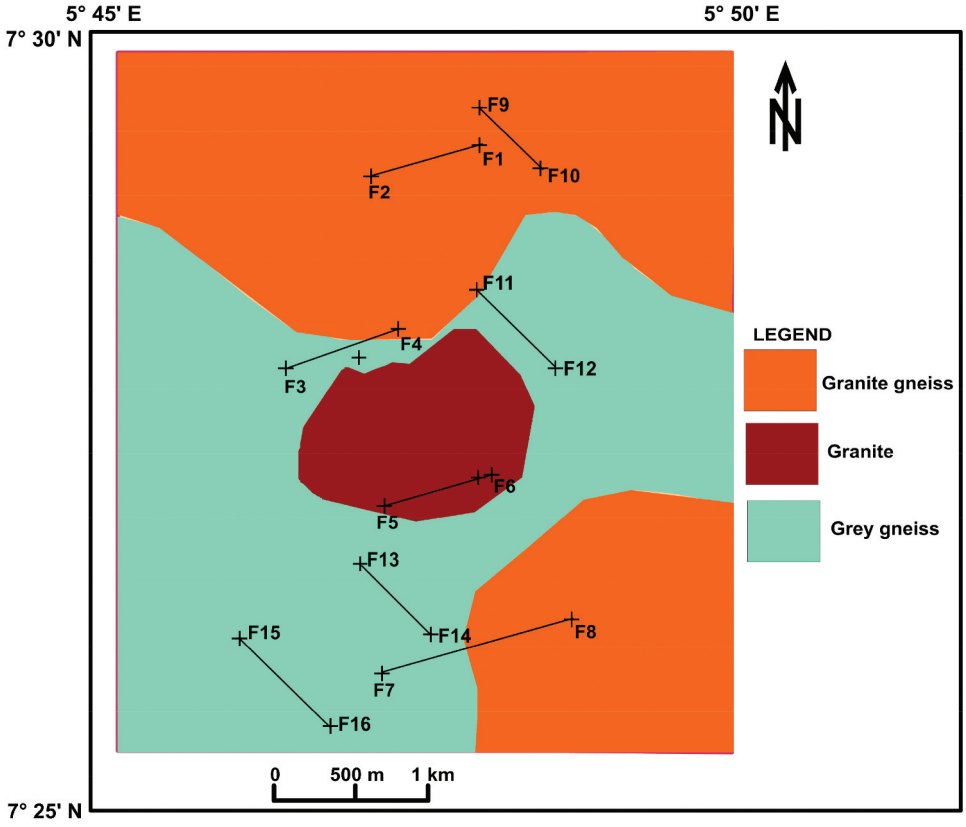

Figure 31. Structural characterisation view of the area.

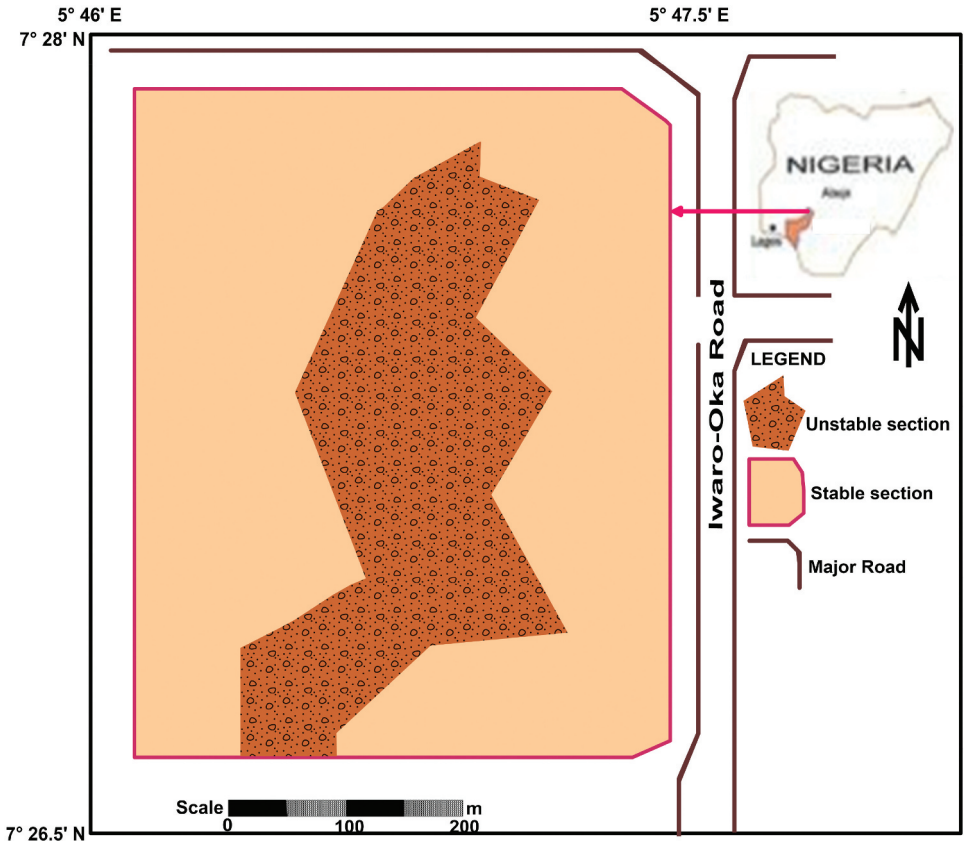

Figure 32. Subsurface Characterisation map of the engineering site.

precautionary measures are not put in place to mitigate possible challenges. Four distinct subsurface layers are delineated. Water saturated clayey subsoil at some points within the site is incompetent layer that cannot sustain civil engineering works. The saturated clayey nature of the subsoil could negatively impact the integrity and stability of building foundation which may extend to the region. Uneven bedrock topography with depressions at some locations could also threaten the foundation stability of the construction works causing differential settlement. This bedrock topography should be taken into consideration in providing appropriate precautionary measures against building failure. The engineering site is categorised into stable and unstable sections; the unstable sections being the incompetent zones would contribute to the failure of proposed construction works hence should be avoided, except proper preventive measures are put in place during foundation design and construction to mitigate future challenges. Failure of engineering structures in the site may arise from the existence of concealed geologic structures: lithologic contact, bedrock depressions, water saturated clayey subsoil, heterogeneous and structurally deformed (F1–F16) subsurface geological setting. Groundwater moves from north to south and northeastern regions to southwestern parts. Thus, structural foundations should be erected towards northeastern and northern sides to prevent water accumulation at base of the foundation. The subsoil at shallow depth of the location is incompetent and unsuitable for foundation; thus, shallow foundation is not encouraged. To avert the risk of structural failure after construction, deep foundations in the form of piers and piles are encouraged except in cases of soil stabilisation for sustainable structural development. Documentation of findings of results of this study is recommended for foundation design, construction of the site and future development of other engineering sites. This study would proffer significant solutions against building failure, guide in engineering investigation for planning, design and construction of new buildings, highway, bridges, dams and other engineering structures. It is also useful for groundwater exploration, environmental studies and forms baseline information for further geophysical investigation in a complex geological terrain. Thus, the techniques serve as invaluable tools efficient for subsurface characterisation for sustainable structural development.

Disclosure statement

No potential conflict of interest was reported by the author(s).

ORCID

Omowumi Ademila http://orcid.org/0000-0001-5177-1110

References

Ademila O. 2015. Integrated geophysical survey for post foundation studies in a typical basement complex of Southwestern Nigeria. The Pacific Journal of Science and Technology. 16(2):274–285.

Ademila O. 2018. Geotechnical influence of underlying soils to pavement failure in Southwestern Part of Nigeria. Malaysian Journal of Sustainable Environment. 4 (1):19–36. doi:10.24191/myse.v4i1.5604.

Ademila O. 2021. Combined geophysical and geotechnical investigation of pavement failure for sustainable construction of Owo-Ikare Highway, Southwestern Nigeria. National Research Institute of Astronomy and Geophysics (NRIAG) Journal of Astronomy and Geophysics. 10(1):183–201. doi:10.1080/20909977.2021.1900527.

Ademila O, Olayinka AI, Oladunjoye MA. 2020. Land satellite imagery and integrated geophysical investigations of highway pavement instability in Southwestern Nigeria. Geology, Geophysics and Environment. 46(2):135–157. doi:10.7494/geol.2020.46.2.135.

Ademila O, Ololade IA. 2018. Geoelectrical imaging and physicochemical assessment of Odokene dumpsite, Nigeria: implications on groundwater quality. Environmental Research, Engineering and Management. 74(3):42–54. doi:10.5755/j01.erem.74.3.21341.

Ademila O, Saloko B. 2018. Hydroelectrical evaluation of groundwater flow pattern in Supare Akoko, Nigeria. Environmental and Earth Sciences Research Journal. 5 (1):7–14. doi:10.18280/eesrj.050102.

Agunloye O. 1984. Soil aggressivity along steel pipeline route at Ajaokuta. Journal of Mining and Geology. 21(1 & 2):97–101.

Baeckmann W, Schwenk W. 1997. Handbook of cathodic protection. In: The theory and practice of electrochemical corrosion protection techniques. 3rd Edition, Elsevier Science Inc, USA. 568p. https://doi.org/10.1016/B978-0-88415-056-5.X5000-X .

Bayrak M. 2002. Exploration of chrome ore in Southwestern Turkey by VLF-EM. Journal of the Balkan Geophysical Society. 5(2):35–46.

Capilleri PP, Massimino MR, Motta E, Todaro M. 2018. Two-dimensional site seismic response analyses for a strategic building in Catania. Annals of Geophysics. 61 (2):1–18. doi:10.4401/ag-7704. SE219, 2018.

Cardarelli E, Cercato M, Di Filippo G. 2007. Assessing foundation stability and soil structure interaction through integrated geophysical techniques: a case history in Rome (Italy). Near-Surface Geophysics. 5(2):141–147. doi:10.3997/1873-0604.2006026.

Chandran D, Anbazhagan P. 2020. 2D non-linear site response analysis of shallow bedrock sites using integrated subsurface profiles. Annals of Geophysics. 63 (4):1–23. doi:10.4401/ag-8326. SE438, 2020.

Dipro for Windows. 2001. DiproTM Version 4.01, Processing and interpretation software for electrical resistivity data. Daejeon (South Korea):Korea Institute of Geosciences and Mineral Resources (KIGAM).

Khalil MA, Abbas AM, Santos FAM, Mesbah HSA, Massoud U. 2010. VLF-EM study for archaeological

investigation of the Labyrinth mortuary temple complex at Hawara area, Egypt. Near Surface Geophysics. 8 (3):203–212. doi:10.3997/1873-0604.2010004.

Loke MH 2000. Electrical imaging surveys for environmental and engineering studies: a practical guide to 2-D and 3-D surveys. p. 61. http://www.heritagegeophysics.com/images/lokenote.pdf .Accessed 15th July, 2020.

Nabighian MN. 1988. Electromagnetic methods in Applied Geophysics, Vol. 1, Theory. In: Society of Exploration Geophysicsists (SEG). Tulsa (OK); p. 528.

Oluwafemi O. 2012. The role of geophysics in the investigation of waste disposal site in Ikare-Akoko area, Southwestern Nigeria. International Journal of Science and Emerging Technologies. 4(5):181–204.

Oluwafemi O, Oladunjoye MA. 2013. Integration of surface electrical and electromagnetic prospecting methods for mapping overburden structures in Akungba-Akoko, Southwestern Nigeria. International Journal of Science and Technology. 2(1):122–147.

Orellana E, Mooney HM. 1966. Master tables and curves for vertical electrical sounding over layered structures. Madrid: Inteciencis; p. 34.

Pazzi V, Tapete D, Cappuccini L, Fanti R. 2016. An electric and electromagnetic geophysical approach for subsurface investigation of anthropogenic mounds in an urban environment. Geomorphology. 273:335–347. doi:10.1016/j.geomorph.2016.07.035.

Pirttijarvi M. 2004. KH filt program. A geophysical software for Karous-Hjelt and Fraser Filtering on Geophysical VLF (very low frequency) Data. Finland: Geophysical Division, Department of Geosciences, University of Oulu.

Rahaman MA. 1989. Review of the basement geology of Southwestern Nigeria. In: Kogbe CA, editor. Geology of Nigeria. Nigeria: Elizabeth Publishing; p. 39–56.

Sharma PV. 1997. Environmental and Engineering Geophysics. Cambridge: Cambridge University Press.

Vander Velper BPA. 2004. WinResist Version 1.0 Resistivity Depth Sounding Interpretation Software. Delft Netherland: M.Sc. Research Project, ITC.

Zohdy AAR. 1965. The auxiliary point method of electrical sounding interpretation and its relationship to dar-zarrouk parameters. Geophysics. 30(4):644–650. doi:10.1190/1.1439636.